

MASSACHUSETTS INSTITUTE OF TECHNOLOGY
LINCOLN LABORATORY

ANALYSIS OF DATA
FROM THE AVON-TO-WESTFORD EXPERIMENT

R. K. CRANE

Group 61

TECHNICAL REPORT 498

8 JANUARY 1973

LEXINGTON

MASSACHUSETTS

The work reported in this document was performed at Lincoln Laboratory, a center for research operated by Massachusetts Institute of Technology. This work was sponsored by the National Aeronautics and Space Administration under Contract NAS 5-21626.

Non-Lincoln Recipients

PLEASE DO NOT RETURN

Permission is given to destroy this document when it is no longer needed.

ABSTRACT

This report describes the analysis of results of a Lincoln Laboratory experiment which consisted of a series of bistatic scatter and radar measurements of the scattering cross section per unit volume of rain and thin turbulent layers. Results of the experiment are presented as average and rms values of the ratio of the bistatic scatter cross section as calculated using the radar data to the cross section as measured with the bistatic scatter system. The goal of the experiment was to test the precision of the approximate description of scattering due to rain and thin turbulent layers used in interference prediction.

The experiment utilized a 143-km scatter path from Avon, Connecticut, to the Westford Communications Terminal that was operated at 7.74 GHz during the summer of 1968 and at 4.515 GHz during the summer and fall of 1970. Simultaneous radar observations were made with the Millstone Hill 1.295-GHz radar in Westford, Massachusetts. Scatter measurements were made using scattering angles that ranged from 2° to 180° . The measurements showed that the approximate descriptions of scattering due to rain and thin turbulent layers adequately describe the scattering process within the maximum calibration uncertainties of both the bistatic scatter system and the radar. The average ratios of calculated-to-measured cross section for scattering by rain were +1.2 dB at 4.515 GHz during the summer of 1970 and -1.6 dB at 7.74 GHz during the summer of 1968. The average ratio of calculated-to-measured cross section for scattering by snow was +2.1 dB measured during the fall of 1970. The average ratio for turbulent scatter was -0.8 dB measured during the fall of 1970. The maximum errors in the estimation of the ratio due to calibration uncertainty were 2.7 dB for the 1970 measurements and 3.7 dB for the 1968 measurements.

CONTENTS

Abstract	iii
I. Introduction	1
II. Brief Experiment Description	3
III. Review of the Approximate Descriptions of Rain and Turbulent Layer Scatter	9
IV. Measurements	14
A. Fall 1970	14
B. Summer 1970	27
C. Summer 1968	33
V. Analysis of Data	35
A. Best Estimate Comparison	35
B. Discussion of Results, Hydrometeor Scatter	39
C. Discussion of Results, Turbulent Scatter	41
VI. Conclusions	43
Acknowledgment	44
References	45

ANALYSIS OF DATA FROM THE AVON-TO-WESTFORD EXPERIMENT

I. INTRODUCTION

Interference between communication systems located beyond each other's radio horizon and operating at the same wavelength in the centimeter or millimeter bands may be caused by one or more of the following propagation phenomena – rain scatter, turbulent layer scatter, ducting, or terrain diffraction. The Avon-to-Westford experiment was conducted to investigate the precision of the approximate descriptions of two of these phenomena – rain scatter and thin turbulent layer scatter – currently used in estimating interference.^{1,2} Simultaneous measurements of scattering from either thin turbulent layers or rain cells were made using the Millstone Hill L-band radar and either an X-band or a C-band bistatic scatter system operated between Avon, Connecticut,* and the Westford Communications Terminal. The monostatic (radar) measurements and the approximate descriptions of the bistatic scattering process were used to compute the expected transmission loss for the bistatic scatter system. The expected and measured transmission loss values were then compared.

The X-band bistatic measurements were made during the summer of 1968 and a report, "A Comparison Between Monostatic and Bistatic Scattering from Rain and Thin Turbulent Layers"³ was issued that described the equipment and a preliminary analysis of the data. The C-band measurements were made during the summer and fall of 1970. A description of the radar and the C-band equipment and a preliminary examination of some of the summer data are given in "Description of the Avon-to-Westford Experiment."⁴ The latter report also discussed the approximate descriptions of the two propagation phenomena of interest and described the method used to compute the expected transmission loss for comparison with the bistatic system measurements. This report provides an analysis of the data from both the C- and X-band experiments. The equipment descriptions are provided in Refs. 3 and 4 and will only be augmented and summarized here.

The X-band measurements were conducted between 29 July and 9 August 1968. During this time period 86 hours of observations were obtained with the bistatic scatter system and 76 hours of observations with the Millstone Hill L-band radar. Approximately 30 percent of these observations were of rain scatter. Most of the rain observations were not useful for comparison because clear lines-of-sight were not present between the antennas and the rain cells. Useful simultaneous measurements were obtained during only four hours of the measurement period. For these measurements, the data showed the computed transmission loss to be 1.6 ± 0.5 dB[†] higher than the measured transmission loss (the measured received signal level was 1.6 dB higher than the computed signal level; the ratio of the calculated-to-measured scattering cross section per unit volume was -1.6 dB).

The C-band measurements were conducted between 20 July and 31 July 1970 and between 26 October and 13 November 1970. During the earlier time period, 61 hours of observations with the bistatic system and 70 hours of observations with the radar system were obtained. Of these observations approximately 30 percent were for rain scatter and, of the rain scatter measurements, approximately 4 hours of useful simultaneous measurements were obtained. For these

* Site provided courtesy of Station WTIC, Hartford, Connecticut.

† That is, the mean of the logarithm of the ratio of computed-to-measured transmission loss is estimated to be 1.6 dB with an uncertainty (3σ) of ± 0.5 dB.

TABLE I
 AVON-TO-WESTFORD X-BAND BISTATIC SCATTER SYSTEM

Frequency	7.74 GHz (3.88-cm wavelength)
Antenna 1	60-foot paraboloid with Cassegrainian feed
Gain Antenna 1	59.4 ± 0.7 dB
Beamwidth Antenna 1	0.15° between half-power points
Polarization Antenna 1	Left-hand circular
Antenna 2	Standard gain horn or 6-foot paraboloid with prime focus feed
Gain Antenna 2	18.2 ± 0.2 dBi for horn 39.5 ± 0.3 dBi for 6-foot paraboloid
Beamwidth Antenna 2	23° for horn 1.5° for 6-foot paraboloid
Polarization Antenna 2	Horizontal for either antenna
Transmitted Power	Variable 1 W to 500 W
Transmitted Signal	CW with frequency stability of 1 part in 10^{10} per day
Receiver	Phase lock
Receiver Bandwidth	560 or 2880 Hz
Receiver Noise Temperature	$\sim 600^\circ\text{K}$ (including atmospheric and ground effects)
Maximum Measurable Transmission Loss	200 dB for horn 220 dB for 6-foot paraboloid
Path Length	143 km
Data Processing	Received signal AGC voltage and local oscillator frequency sampled 20 times per second

measurements, the computed transmission loss was 1.2 ± 0.4 dB lower than the measured transmission loss. For 38 elevation scans obtained during the fall of 1970 series of measurements, the computed transmission loss was 2.1 ± 0.7 dB lower than the measured value. These comparisons between the estimated and measured transmission loss values for hydrometeor scatter show that within the 3.7 dB combined measurement accuracy of both the radar and bistatic scatter systems for 1968 and the 2.7 dB combined measurement accuracy for 1970, the simple Rayleigh scattering theory for spheres when applied to scattering by hydrometeors provides an adequate estimate of the transmission loss.

Simultaneous measurements of thin turbulent layer scatter were made throughout each measurement period. Radar data obtained between 1440 and 1630 GMT on 2 November 1970 were free of cloud and ground clutter contamination for heights below 5 km. A comparison between the bistatic measurements and radar estimates for this time period shows the ratio of estimated-to-measured transmission loss to be 0.8 ± 1.2 dB. The data indicate agreement between prediction and measurement within the measurement accuracy of the bistatic scatter and radar systems.

The magnitudes of the means of the logarithms of the ratios of measured-to-computed transmission loss for measurements of scattering by rain or snow are smaller than the maximum possible measurement error for each of the measurement periods. The rms fluctuations in the logarithm of the ratios were, for the clear lines-of-sight cases, 3.7 dB for the C-band measurements made during the summer of 1970 and 3.2 dB for the X-band measurements made during the summer of 1968. These values compare favorably with the estimated 3.2 dB rms value based upon an analysis of the equipment and measurement techniques used (see Table V, Ref. 4). Although the estimate of the mean of the logarithm of the ratio of measured-to-computed transmission loss is within the maximum possible equipment calibration error, the actual calibration error is most likely to be smaller and the differences may be significant. A possible reason for the observed difference is the use of Rayleigh scattering theory for dielectric spheres in the calculations. The hydrometeors are, in general, not spherical and the exact (Mie) scattering cross section for spheres is slightly different from the Rayleigh estimate. Computations based upon Rayleigh scattering from spheroidal particles bring the C-band measurements and calculations into closer agreement (see Section V. B.). Computations based upon exact theory for spheres bring the X-band measurements and calculations into closer agreement. The use of the simple Rayleigh scattering theory for dielectric spheres does, however, allow prediction of the transmission loss within 2 dB for the combinations of transmitter and receiver polarization used.

II. BRIEF EXPERIMENT DESCRIPTION

The bistatic scatter and radar systems used for the three experiment periods, summer of 1968, summer of 1970, and fall of 1970 are described in Refs. 3 and 4. A brief summary of the equipment parameters are given in Tables I to III. Table IV presents a summary of the measurement accuracies of each of the systems. The accuracy estimates for the X-band system are derived from the values given in Ref. 4 for the C-band system. The larger error in the ratio of estimated-to-measured transmission loss for the X-band system reflects the uncertainty in the calibration of the variable attenuator inserted between the antenna and receiver to increase the dynamic range of the Millstone Hill L-band radar. The accuracy, repeatability, and precision values given in Table IV describe the possible difference between the measurements made by each system and measurements made with an ideal, error-free system for all the measurements made (accuracy), the additional possible difference for measurements made during a single scan

TABLE II
AVON-TO-WESTFORD C-BAND BISTATIC SCATTER SYSTEM

Frequency	4.515 GHz (6.644-cm wavelength)
Antenna 1	60-foot paraboloid with Cassegrainian feed
Gain Antenna 1	55.5 ± 0.7 dB
Beamwidth Antenna 1	0.2° between half-power points
Polarization Antenna 1	Vertical
Antenna 2	4-foot paraboloid with prime focus feed Standard gain horn
Gain Antenna 2	32.8 ± 0.3 dB for 4-foot paraboloid 18.1 ± 0.1 dB for horn
Beamwidth Antenna 2	3.5° for 4-foot paraboloid 22° for horn
Polarization Antenna 2	Vertical for either antenna
Transmitter Power	Variable 1 W to 1 kW
Transmitted Signal	CW with frequency stability of 1 part 10^{10} per day
Receiver	Phase lock
Receiver Bandwidth	560 and 2880 Hz
Receiver Noise Temperature	$\sim 2000^\circ\text{K}$
Maximum Measurable Transmission Loss	190 dB
Path Length	143 km
Data Processing	Received signal AGC voltage and local oscillator frequency sampled 20 times per second

TABLE III
MILLSTONE HILL L-BAND RADAR

	Summer 1968	Summer and Fall 1970
Frequency	1.295 GHz (23.2-cm wavelength)	1.295 GHz
Antenna	84-foot paraboloid with Cassegrainian feed	
Antenna Gain	47.2 ± 0.3 dB	46.7 ± 0.3 dB
Beamwidth	0.7°	0.7°
Polarization	Right-hand circular transmit, left-hand circular receive	
Transmitted Power	3.3 MW peak	3.3 MW peak
Pulse Length	10.0 μsec	12.4 μsec
Pulse Repetition Rate	120 per second	120 per second
Receiver Bandwidth	80.5 kHz	80.5 kHz
Data Processing	Analog-to-digital conversion of the IF sine and cosine channels every 10 μsec	
Computer Sampling Rate	20 per second	20 per second
Detection	Square law by computer operations	
Dynamic Range	40 dB*	80 dB
System Noise Temperature	280°K	280°K
System Line Losses (transmit and receive)	2.2 dB	2.8 dB
Matched Filter Processing Loss	1.4 dB	1.1 dB
Single Pulse Z_e Value for Unity Signal-to-Noise Ratio	-30 dBZ† at 100 km	-30 dBZ at 100 km
<p>* Increased to 80 dB by a manually adjusted variable attenuator in the transmission line between the antenna and receiver.</p> <p>† dB relative to $Z = 1 \text{ mm}^6/\text{m}^3$.</p>		

TABLE IV
MEASUREMENT ACCURACIES

Measurement	Accuracy (dB)	Repeatability ¹ (dB)	Precision ² (dB)
L-band radar Measurement of Z_e - 1970 ³	1.4	0.2	0.7
L-band radar Measurement of Z_e - 1968 ⁴	2.4	0.2	0.7
C-band bistatic scatter system Measurement of L ⁵	0.4	0.8	1.7
X-band bistatic scatter system Measurement of L ⁵	0.4	0.8	1.7
Ratio of estimated-to-measured transmission loss ⁶ for C-band system, Summer and Fall 1970	2.7	3.2	1.8
Ratio of estimated-to-measured transmission loss ⁷ for X-band system, Summer of 1968	3.7	3.2	1.8

Notes:

1. Accuracy and repeatability are reported as the maximum possible uncertainty (equivalent of 3 standard deviations for a Gaussian process).
2. Precision is reported as an rms value (equivalent of 1 standard deviation for a Gaussian process).
3. From β_B , Table IV, Ref. 4.
4. Accuracy value is increased by 1 dB due to an uncertainty in the calibration of the attenuator used to increase receiver dynamic range.
5. From (P_r/P_t) , Table II, Ref. 4. This value is used for both the X- and C-band systems since the receiver systems were identical.
6. From all data, horn, Table V, Ref. 4.
7. From all data, horn, Table V, Ref. 4 with the accuracy estimate increased by 1 dB due to attenuator calibration uncertainty.

(repeatability), and the additional possible difference for a single 2.5-sec average radar measurement or 6-sec average bistatic scatter system measurement (precision).

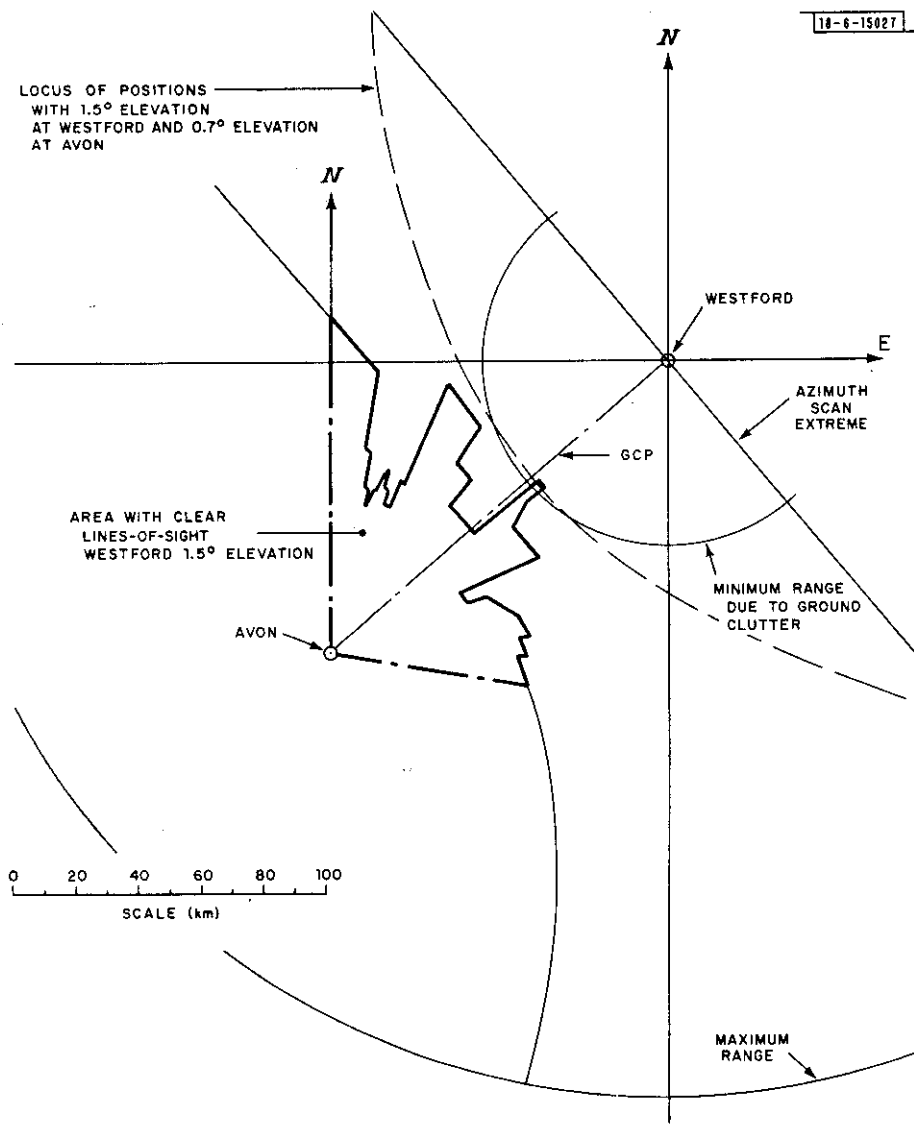
The scatter path used for the bistatic measurements is shown in Figs. 11 and 12 of Ref. 4. The transmitter foreground is depicted in Fig. 13 of Ref. 4. The receiver foreground is not depicted but, for all azimuthal angles between 140° and 240° and between 250° and 280° , the L-band radar and the X- or C-band bistatic scatter system receiver antenna patterns within the receiver resolution volume polar angle are above the local horizon for a 1° elevation angle. (See Fig. 8, Ref. 4, the X-band system resolution volume polar angle is smaller than shown in Fig. 8.) The antenna beams are above the local horizon for all azimuth angles between 140° and 320° at elevation angles greater than and equal to 1.5° . Using the angular position of the tops of the trees shown in Fig. 13 of Ref. 4 to define the local horizon at Avon, the area having clear lines-of-sight from the transmitter to the scatterer to the receiver is depicted in Fig. 1 for a 1.5° elevation angle at Westford. The area was computed using spherical geometry and a 1.23 effective earth radius to correct for refraction.

Figure 2 of Ref. 4 shows the transmitter van in position and the obstructions behind the transmitter. For azimuth angles between 100° and 360° relative to the transmitter, two rows of trees provide obstructions up to 60° elevation angle. These obstacles limit the area for useful comparison measurements as shown by the heavy dot dashed lines in Fig. 1. The radar ground clutter is excessive out to a range of 60 km and, at elevation angles above 1.5° relative to the Westford receiving antenna, the 60 km minimum measurement range limits the area for useful comparison.

During the summer of 1968 and the summer of 1970, rain scatter measurements were made whenever rain was detected at ranges in excess of 60 km from the Westford, Millstone Hill antenna complex. The measurements were made by pointing the transmitting horn antenna in the direction of the largest rain cells and scanning the Westford and Millstone Hill antennas in azimuth at a fixed elevation angle (azimuth scan) over a range of azimuth angles including the rain cells. The Westford and Millstone Hill antennas were scanned at a constant angular rate with both antennas pointed in the same direction. During the fall of 1970 the measurement scheme was modified to make elevation scans at fixed azimuths rather than azimuth scans at fixed elevation angles.

Turbulent scatter measurements were made using either the horn or dish antennas (4-foot paraboloid at C-band or 6-foot paraboloid at X-band) to illuminate the great circle path and elevation or azimuth scans with the Westford antenna. The Millstone Hill radar made only elevation scans when turbulent layer scatter was being observed. The Westford and Millstone Hill antennas were scanned in synchronism (pointing at the same elevation and azimuth angle) only for the turbulent layer measurements made during the fall of 1970.

Additional weather radar data were provided by an on-site S-band AN/FPS-18 radar, by the C-band AN/FPS-77 weather radar operated by the Air Weather Service at Hanscom Field, and by the S-band AN/FPS-66 weather radar operated by the Weather Radar Research Project of the Department of Meteorology at M. I. T. These additional data were used to position the observation volumes for the Millstone Hill L-band radar and the bistatic scatter systems and to ascertain whether rain occurred within the 60 km ground clutter range to the Westford, Millstone Hill antenna complex. In addition, the Air Weather Service at Hanscom Field provided K_a -band AN/TPQ-11 cloud radar data for use in assessing the vertical profiles of clouds and turbulent layers and the Air Force Cambridge Research Laboratory (AFCLR) provided special radiosonde measurements for determining temperature and wind profiles during the measurement program.



C61-1111

Fig. 1. Area for clear lines-of-sight, Westford antenna at 1.5° elevation angle.

During the three measurement periods, AFCRL provided between 1 and 2 special radiosonde flights per day for use in post test analysis.

III. REVIEW OF THE APPROXIMATE DESCRIPTIONS OF RAIN AND TURBULENT LAYER SCATTER

Bistatic scatter from rain and thin turbulent layers may, for the X- and C-band frequencies used in this experiment, be described by single scattering theory.^{5,6} Using single scattering theory, Rayleigh scattering theory to describe scattering from hydrometeors, and assuming that the scatterers are spherical, the transmission loss for a bistatic scatter system may be computed when the spatial distribution of hydrometeors is known. Reference 5 provides a detailed derivation of the bistatic radar equation for scattering by rain. Equation (22) of Ref. 5 provides the usual starting place for the derivation of an approximate expression for transmission loss. This equation is identical to Equation (1) of Ref. 4 after correction as indicated in the errata sheet with the exception of the integration over the drop size distribution. The starting equations are reproduced here for ease of reference:

$$\frac{P_r}{P_t} = \frac{1}{L} = \frac{G_1 G_2 l_1 l_2 \lambda^2}{(4\pi)^3} \int_{Vol} g_1 g_2 \beta(\underline{x}) \frac{d\underline{x}}{x^2 \rho^2} 10^{-(1/10) \left[\int_0^{\underline{x}} \alpha ds + \int_{\underline{x}}^{\underline{d}} \alpha ds \right]} \quad (1)$$

$$\beta(\underline{x}) = \frac{4\pi}{k^2} \int |\hat{u}_1 \cdot \underline{S}(a, \epsilon, \underline{x}) \cdot \hat{u}_2|^2 \bar{\eta}(a, \underline{x}) da \quad (2)$$

$$\underline{\rho} = \underline{d} - \underline{x}$$

where

L = transmission loss

P_r = received power

P_t = transmitted power

G_1 = receiver antenna gain

G_2 = transmitter antenna gain

l_1, l_2 = receiver and transmitter losses (factor < 1)

λ = wavelength

g_1, g_2 = normalized radiation pattern of the receiver and transmitter antennas (directivity)

β = scattering cross section per unit volume

$\underline{x}, \underline{\rho}$ = position vectors of magnitude x and ρ , respectively

\underline{d} = position of receiver relative to transmitter (or vice versa)

$k = 2\pi/\lambda$

\underline{S} = scattering amplitude tensor for a hydrometeor of dielectric constant ϵ and shape parameter a

$\bar{\eta}$ = average number density (number per unit volume per unit a)
of hydrometeor scatterers of parameter a

\hat{u}_1, \hat{u}_2 = unit vectors describing the polarization properties of the transmit
and receive antennas (unit vectors in the direction of the electric
field vector)

α = specific attenuation (dB/km).

The equations given in Ref. 4 are correct when the expression $\hat{u}_1 \cdot \hat{\underline{s}} \cdot \hat{u}_2$ in the report as originally published or the expression $|\hat{u}_1 \cdot \hat{\underline{s}} \cdot \hat{u}_2|^2$ in the report as corrected by the errata sheet is changed to $\beta(\underline{x})$ as given in Eq. (2) above. The equations presented in Ref. 4 are for $\alpha = 0$ or no attenuation. Equation (7) of Ref. 4 gives the expression for $\beta(\underline{x})$ for Rayleigh scattering by dielectric spheres and is repeated here after correction.

$$\beta(\underline{x}) = |\hat{u}_1 \cdot (\hat{a}_1 \cos \varphi \hat{a}_2 + \hat{b}_1 \hat{b}_2) \cdot \hat{u}_2|^2 \frac{\pi^5 Z(\underline{x}) |\kappa|^2}{\lambda^4} \quad (3)$$

where

\hat{a}_1, \hat{a}_2 = unit vectors in the plane of scattering (plane including transmitter,
receiver, and \underline{x})

\hat{b}_1, \hat{b}_2 = unit vectors perpendicular to the plane of scattering

φ = scattering angle

$|\kappa|^2 = |(\epsilon - 1)/(\epsilon + 2)|^2$, ϵ = dielectric constant for hydrometeor

$$Z(\underline{x}) = \int_a (2a)^6 \bar{\eta}(a, \underline{x}) da$$

a = dielectric sphere radius.

Using these equations, assuming that attenuation may be neglected as was done in Ref. 4, and noting that the scattering volume is defined by the receiver antenna and the rain cell along the receiver antenna beam,

$$\frac{1}{L} = A_R G_2(\hat{\rho}) |\hat{u}_1 \cdot (\hat{a}_1 \cos \varphi \hat{a}_2 + \hat{b}_1 \hat{b}_2) \cdot \hat{u}_2|^2 \frac{ZD}{\rho^2} \quad (4)$$

where

$$A_R = \frac{\pi^2 |\kappa|^2}{64 \lambda^2} G_1 \int_0^{\Omega_m} g_1(\Omega) d\Omega \cdot 10^{-17}$$

when Z is expressed in mm^6/m^3 ; D, ρ in km; λ in cm; Ω_m is the resolution solid angle (see Fig. 8, Ref. 4); and D is a distance that defines the effective volume along the beam that is occupied by the scatterers. (See Eq. (3) of Ref. 4.) For thin turbulent layer scatter, the equation for $\beta(\underline{x})$ is given by (Eq. 10, Ref. 4 after correction):

$$\beta(\underline{x}) = |\hat{u}_1 \cdot (\hat{a}_1 \cos \varphi \hat{a}_2 + \hat{b}_1 \hat{b}_2) \cdot \hat{u}_2|^2 \frac{0.378 C_n^2(\underline{x})}{\lambda^{1/3} (\sin \varphi/2)^{11/3}} \quad (5)$$

and the approximate expression for transmission loss as given by (Eq. 11, Ref. 4):

$$\frac{1}{L} = A_T G_2(\hat{\rho}) |\hat{u}_1 \cdot (\hat{a}_1 \cos \varphi \hat{a}_2 + \hat{b}_1 \hat{b}_2) \cdot \hat{u}_2|^2 \frac{C_n^2 D}{\rho^2} (\sin \frac{\varphi}{2})^{-11/3} \quad (6)$$

where

C_n^2 = the structure constant,² a meteorological parameter that describes the intensity of random fluctuations of the index of refraction of the clear atmosphere in the inertial subrange

and

$$A_T = \frac{1.76\lambda^{5/3}}{(4\pi)^3} G_1 \int_0^{\Omega_m} g_1(\Omega) d\Omega \cdot 10^{-7}$$

= when C_n^2 is expressed in $m^{-2/3}$, λ in cm and D, ρ in km.

For ease of reference and to make the form of Eqs. (3) through (6) identical with the form of the equations used in Refs. 1 and 5, the polarization mismatch factor, m , may be introduced,

$$m = |\hat{u}_1 \cdot (\hat{a}_1 \cos \varphi \hat{a}_2 + \hat{b}_1 \hat{b}_2) \cdot \hat{u}_2|^2 \quad (7)$$

Equation (4) provides the approximate description of rain scatter used by the International Radio Consultative Committee (CCIR)¹ in the preparation of procedures for determining the possibility of interference between different communication systems. The goal of the Avon-to-Westford Experiment was an experimental determination of the error involved in using these equations. The measurement program provided radar estimates of the distribution of $Z(x)$ and direct bistatic measurements of the transmission loss, L . The remaining factors in Eq. (4) are known from either the radar measurements or were assumed from Rayleigh and single scattering theory. The differences between the measured transmission loss and the values computed using Eq. (4) can be either due to calibration errors in either the radar or the bistatic scatter systems or an inadequacy of the assumptions. Although Eq. (6) does not represent a description currently used in interference predictions, it was also tested because of the parallel formalism to the equation for rain scatter, the availability of data, and the hope it may provide a better basis for the prediction of tropospheric scatter due to turbulence than the one currently used by the CCIR.¹

The equation relating the received power obtained with a radar for a particular range resolution cell to the per unit volume scattering cross section of either rain or atmospheric turbulence may be obtained from Eq. (1) by letting antennas 1 and 2 be the same and introducing the limitation to the scattering volume provided by the radar pulse. The general form of this equation is given by Eq. (6) of Ref. 4 and, for measurements of either rain or turbulent scatter, Eqs. (13) and (14) of Ref. 4 provide the relationships between the equivalent reflectivity or the equivalent structure function, the equipment parameters, and the reported measurements, $P_r r_1^2$. The equivalent reflectivity, Z_e , or the equivalent structure constant, C_{ne}^2 , provide a means of expressing the measured radar cross section in terms of a cross section per unit volume and the estimated meteorological parameters, Z or C_n^2 . To express the measured cross section in these terms, prior knowledge must be available about the physical state of the scatterers. For hydrometeors, the scatterers must be spherical rain drops of a known temperature. Since generally neither the state nor the temperature of the hydrometeors is known, the equivalent Z value, Z_e , is formally

computed using the equations for spheres of water at a convenient temperature (0°C) with Z the unknown. In a similar fashion, the equivalent structure constant, C_{ne}^2 , may be formally defined and used as a measure of the scattering cross section per unit volume.

The equation for Z_e is given by (Eq. 13, Ref. 4)

$$\begin{aligned} Z_e &= \left(\frac{\lambda^2 10^{17}}{\pi^5 |\kappa|^2 C_R P_t d} \right) P_r r_1^2 \quad (\text{mm}^6/\text{m}^3) \quad (8) \\ &= 7.43 \times 10^8 P_r r_1^2 \quad (1970) \\ &= 5.40 \times 10^8 P_r r_1^2 \quad (1968) \end{aligned}$$

where

$$d = \frac{c\tau}{2} \quad \text{with } \tau = \text{pulse length and } c = \text{velocity of light,}$$

$$C_R = \frac{\lambda^2 G_1^2}{(4\pi)^3} \int_0^\Omega g_1^2(\Omega) d\Omega = 5.67 \quad (\text{m}^2) \quad ,$$

P_r is in watts, and r_1^2 is in km. The expression for C_{ne}^2 is given by

$$C_{ne}^2 = 1.612 \times 10^{-13} Z_e \quad (\text{m}^{-2/3}) \quad . \quad (9)$$

The constants in Eqs. (8) and (9) are found from the values listed in Table III and Eq. (9) holds only at the 1.295 GHz radar frequency due to the differences in frequency dependence of the scattering processes as given in Eqs. (3) and (4).

The equation for transmission loss used to compute the expected value for comparison with the measured value is, from Eq. (15), Ref. 4,

$$\frac{1}{L} = A_R \sum_i G_2(\hat{\rho}_i) M_i Z_{e_i} \frac{d}{\rho_i} \quad (10)$$

where A_R is given by Eq. (4), M_i is the polarization mismatch given by Eq. (7), and a summation of the contributions reported by the radar for each range cell (i) of length d along the beam is used instead of the cell defined length D given in Eq. (4). From the definition of D , Eq. (3), Ref. 4,

$$D = \frac{\int \beta(\underline{x}) d\underline{x}}{\beta(\underline{x}_1)} = \frac{\sum_i Z_i d_i}{Z(\underline{x}_1)} \quad ,$$

$$\sum_i Z_i d_i = Z(\underline{x}_1) D$$

and Eq. (10) is identical to Eq. (4).

Using the values in Tables I to III, the transmission loss for rain is

$$\frac{1}{L} = \left[\sum_{i=1} \frac{g_2(\hat{\rho}_i) Z_{e_i} M_i}{\rho_i^2} \right] C \quad (11)$$

where

$$\begin{aligned} C &= 5.152 \times 10^{-16} \quad , \quad 4\text{-foot antenna, C-band (1970)} \\ &= 1.746 \times 10^{-17} \quad , \quad \text{horn antenna, C-band (1970)} \\ &= 8.43 \times 10^{-15} \quad , \quad 6\text{-foot antenna, X-band (1968)} \\ &= 6.25 \times 10^{-17} \quad , \quad \text{horn antenna, X-band (1968).} \end{aligned}$$

The transmission loss for turbulent layer scatter was similarly computed using

$$\frac{1}{L} = \left[\sum_{i=1} \frac{g_2(\hat{\rho}_i) M_i}{(\rho_i)^2} \left(\frac{C_{ne_i}^2}{1.612 \times 10^{-13}} \right) \left(\sin \frac{\varphi_i}{2} \right)^{-11/3} \right] C \cdot F \quad (12)$$

where

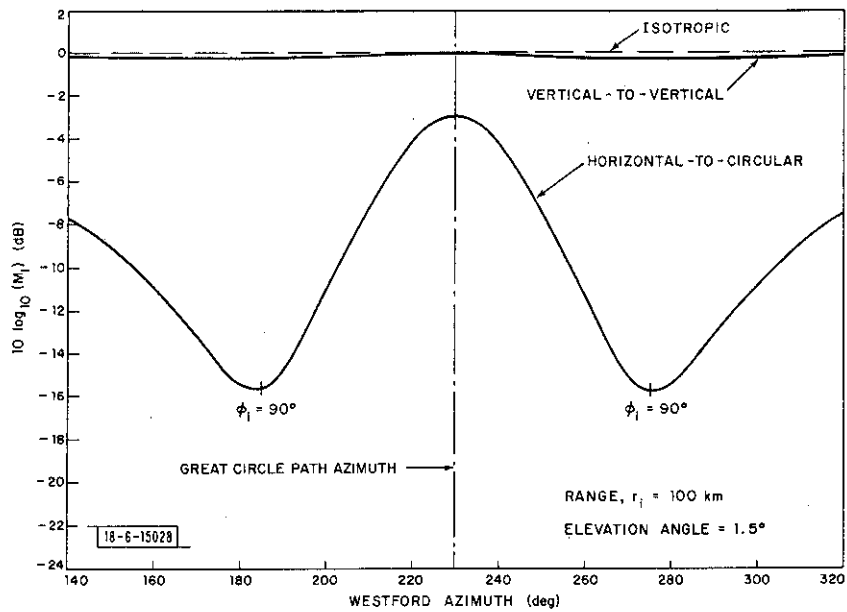
$$\begin{aligned} F &= 0.0128 \quad \text{C-band (1970)} \\ &= 1.009 \quad \text{X-band (1968).} \end{aligned}$$

Since the quantity $(C_{ne_i}^2/1.612 \times 10^{-13})$ is identical to Z_{e_i} [see Eq. (9)], Eqs. (11) and (12) show that the predictions of transmission loss for rain and for turbulent layers differ only by the $(\sin \varphi_i/2)^{-11/3}$ factor and a constant factor, F. This is true only for Rayleigh scatter with the polarization mismatch factor given by Eq. (7).

The combinations of transmitter and receiver polarizations used for the X-band and C-band measurements were different. For the C-band measurements both the transmitting and the receiving antennas were vertically polarized. The X-band measurements were conducted with the transmitting antenna horizontally polarized and the receiving antenna left-hand circularly polarized. The polarization mismatch factor was computed for both the X-band and the C-band polarization combinations by calculating the Cartesian components of each of the vectors indicated in Eq. (7) and forming the dot products. The Cartesian coordinate system had its origin at the scatterer, with \hat{x} directed due south, \hat{y} due east, and \hat{z} vertical. The polarization vectors for each of the antennas were transformed to this coordinate system from similar coordinate systems centered at each antenna using a series of Euler angle rotations⁷ to keep track of the spherical geometry for propagation over the earth. The equations for each of the required vectors are given in Sec. 5, Ref. 4. The polarization vector for the circularly polarized X-band receiving antenna is expressed as

$$\hat{u}_i = \frac{1}{\sqrt{2}} (\hat{v}_r + i\hat{h}_r)$$

where \hat{v}_r and \hat{h}_r are the unit polarization vectors for vertical and horizontal polarization, respectively, for the Westford antenna and $i = \sqrt{-1}$. Using these equations, the polarization mismatch factors for vertical-to-vertical and for horizontal-to-circular polarization are given in Fig. 2



661-1112

Fig. 2. Polarization mismatch factor for vertical-to-vertical and horizontal-to-circular polarization.

for azimuth angles of the scattering locations relative to the Westford site varying from 140° to 320° , the elevation angle fixed at 1.5° , and r_i equal to 100 km. The figure also shows the isotropic scatter idealization. The vertical-to-vertical polarization mismatch is within 0.25 dB of the isotropic idealization for the range of geometrical configurations used in the experiment. For the horizontal-to-circular polarization case, a considerably higher transmission loss is obtained (less signal received) than for isotropic scatter and linear-to-circular polarization (-3 dB). The horizontal-to-circular polarization case provides less transmission loss than horizontal-to-horizontal for a scattering angle of 90° due to the small vertical component of the incident field present at the scatterer.

IV. MEASUREMENTS

A. Fall 1970

During the fall 1970 measurement period data were acquired using elevation scans. Both the Millstone Hill radar and the Westford 60-foot antenna were scanned so both antennas were pointed at the same elevation and azimuth at the same time. Measurements were made during normal working hours on 10 days between 26 October 1970 and 13 November 1970. The weather was clear on three of the days, 27, 28, and 29 October, overcast on 12 November, and was overcast with intermittent light rain, drizzle, and fog on the remaining six days, 26 October, 2, 5, 10, 11, and 13 November. On days with rain or drizzle, the melting layer varied in height from 1.3 to 2.7 km. Scattering was observed from turbulence, cloud particles, and hydrometeors. The hydrometeor type responsible for most of the scatter observations was snow above the melting layer. The cloud particle type observed was ice crystal in thick cirrus (cirrostratus) cloud layers. The scatterers observed were generally horizontally stratified being either turbulent layers, cloud layers, or widespread rain. The scattering cross section per unit volume for these layers changes relatively slowly in the horizontal direction and relatively rapidly in the vertical direction. For this reason, the elevation scan mode of observation was used.

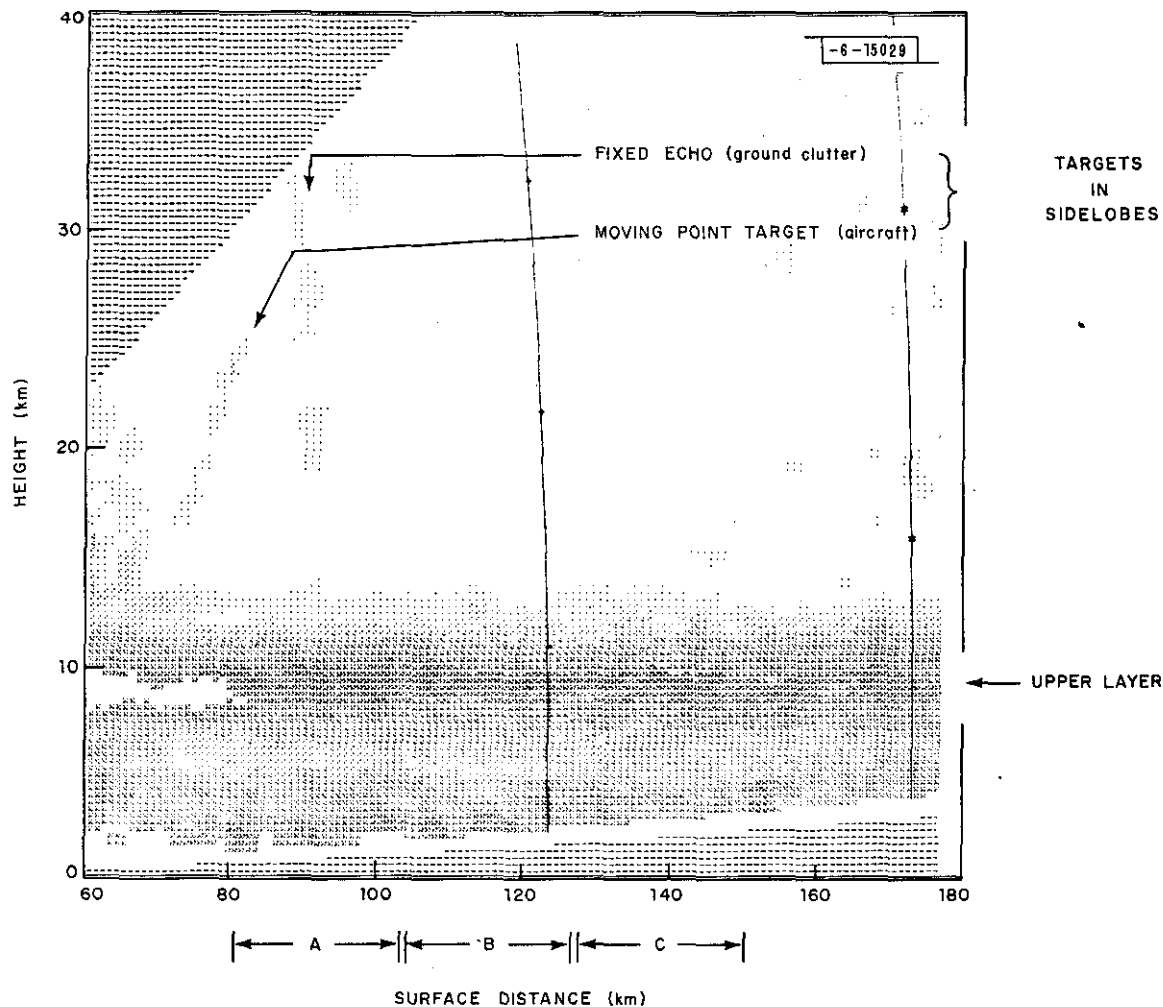


Fig. 3. RHI display Millstone Hill radar, 229.5° azimuth, 1446-1450 GMT, 2 November 1970.

The weather on 2 November 1970 was typical of much of the entire fall 1970 measurement period, overcast changing to drizzle then to intermittent light rain. Millstone Hill L-band radar observations for the time period 1446-1450 GMT (0946-0950 local time) are presented in a computer generated range height indicator (RHI) display on Fig. 3. The observations were made at an azimuth of 229.5° which is within 0.1° of the great circle path between Avon and Westford. The scattering cross section per unit volume is indicated by the shade of each elemental display area (0.3 km × 0.9 km). One dot in a display area indicates that the equivalent Z value was between -30 and -25 dBZ* ($1.6 \times 10^{-16} \text{ m}^{-2/3} \leq C_{ne}^2 \leq 5.1 \times 10^{-16} \text{ m}^{-2/3}$) and each additional dot represents a 5 dB higher value. For a Z_e value greater than $1 \text{ mm}^6/\text{m}^3$, the dots were not displayed. The upper layer is blank at a height of 9 km for surface distances between 60 and 80 km indicating a Z_e value greater than 0 dBZ. The data depicted in Fig. 3 show little change with surface distance. The horizontal stratification of the data is also shown in Fig. 4. The data displayed in Fig. 3 were horizontally averaged over a 22.5-km surface distance interval and plotted vs height in Fig. 4. The horizontal intervals used are indicated by A, B, and C on Fig. 3.

*dB relative to $Z_e = 1 \text{ mm}^6/\text{m}^3$.

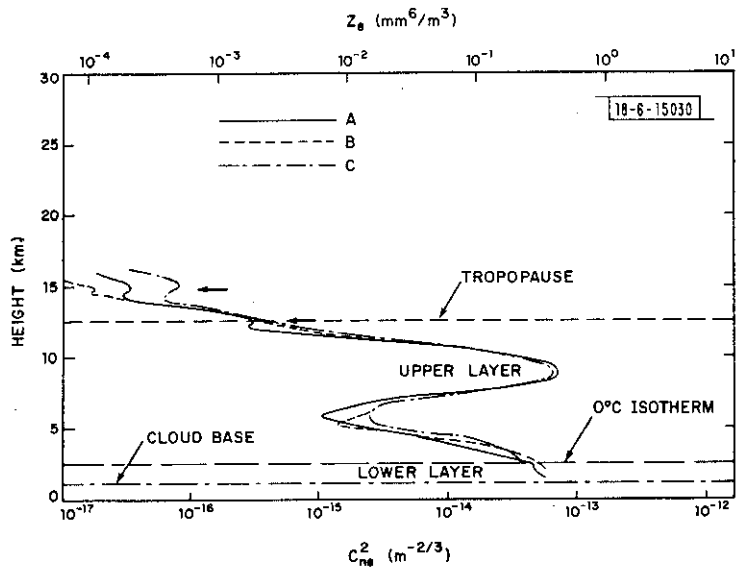


Fig. 4. C_{ne}^2 profile, Millstone Hill radar, 229.5° azimuth, 1446-1450 GMT, 2 November 1970; Avon: 3° elevation, 49° azimuth, 4-foot antenna, vertical polarization.

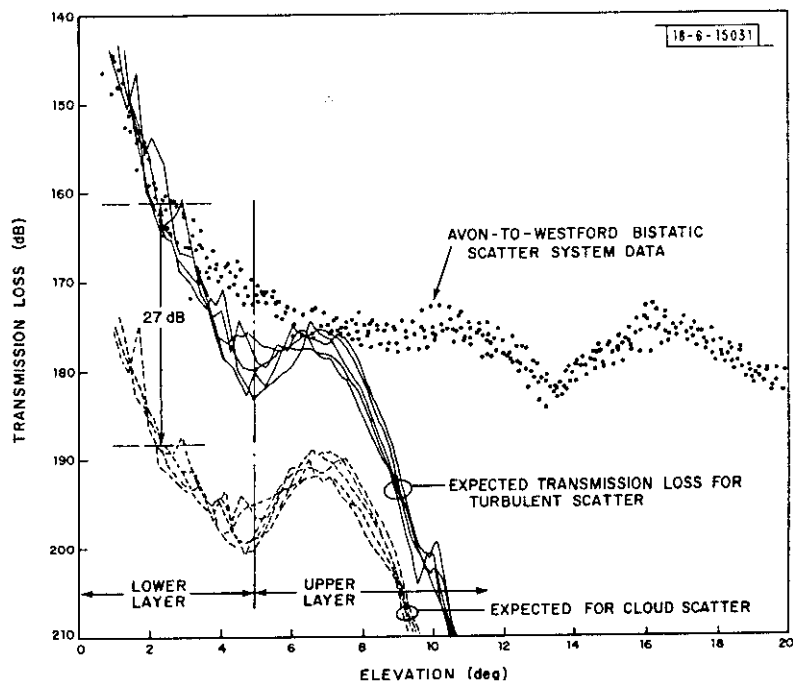


Fig. 5. Calculated and measured transmission loss, Avon-to-Westford scatter path, 229.5° azimuth (Westford), 1446-1456 and 1510-1517 GMT, 2 November 1970; Avon: 3° elevation, 49° azimuth, 4-foot antenna, vertical polarization.

Two strong layers are evident in the data and are labeled the upper and lower layers. The data also show two layers above 10 km which are indicated by short horizontal arrows. Both layers above 10 km are caused by turbulence and the lower one is at the height of the tropopause. The layer labeled as upper corresponds to visually observed (from aircraft) cirrostratus cloud. The lower layer coincided with a visually observed low stratus cloud. The 0°C isotherm and cloud base shown on the figure were obtained from a radiosonde observation made at Hanscom Field approximately three hours later (1800 GMT). The high turbulent layers are readily identified as turbulent because they are situated in a cloud free region. The cause of the lower layers labeled upper and lower is more difficult to ascertain from the radar data alone because the layers may be caused by the observed clouds, by turbulence within the clouds, or by both. Cirrostratus clouds often have reflectivities of greater than $1 \text{ mm}^6/\text{m}^3$ (Ref. 8). The identification of the upper layer as caused by cirrostratus cloud, therefore, is reasonable although simultaneous U-2 aircraft, Millstone Hill L-band radar observations⁹ often showed turbulent layers within cirrostratus clouds. The lower cloud layer is in a much warmer region of the troposphere and is composed of water particles. The Z_e value for water clouds is typically -30 to -20 dBZ. Clouds producing large droplets may, however, have Z_e values of -5 dBZ as observed at the peak of the lower layer. Since a number of turbulent layers below 5 km could also produce the profiles given in Fig. 4, the cause of the lower layer may not be determined without additional data.

Transmission loss data obtained from the Avon-to-Westford bistatic scatter system simultaneously with the data shown in Figs. 3 and 4 and over the following half hour period are shown by the dots on Fig. 5. Each dot represents a 6-second average of the received power and corresponds to a measurement made with the radar system. The expected transmission loss values computed from the radar data using either Eq. (11) for rain or clouds or Eq. (12) for turbulence are shown by the dashed and solid lines, respectively, for each elevation scan. The scans were made along the great circle path. Figure 6 shows the positions of the antenna beams during an elevation scan along the great circle path for the Avon antenna and pointing angles used for obtaining the transmission loss data given in Fig. 5. The heights corresponding to the minimum Z_e or C_{ne}^2 values

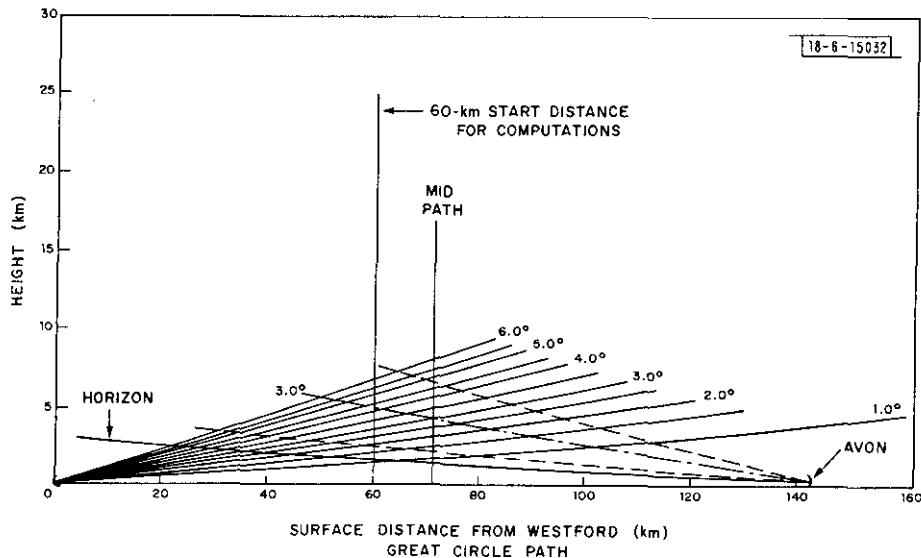


Fig. 6. Antenna beam positions in the great circle plane, Avon-to-Westford scatter path.

between the two layers are between 5 and 6 km and from Fig. 6 correspond to Westford elevation angles between 2.5° and 5° depending upon the surface distance. The expected transmission loss values show that the maximum transmission loss values corresponding to the Z_e or C_{ne}^2 minima occur at elevation angles between 4° and 5° .

The transmission loss values computed assuming that the lower layer was caused by turbulence are in good agreement with the measured values for Westford elevation angles below 2.5° . A comparison between each 6-second average transmission loss measurement and the calculated transmission loss value obtained from simultaneous radar measurements using Eq. (12) (turbulence) for elevation angles below 2.5° shows the average of the ratio of the measured-to-computed transmission loss (computed-to-measured received power) is 0.7 ± 1.8 dB (-0.1 ± 1.8 dB after correction, see Section V). At elevation angles above 2.5° , coupling via the sidelobes of the Westford antenna provides the dominant contribution to the required signal. Sidelobe coupling was generally detected using Doppler shift measurements (see below). Calculations based upon the hypothesis that the lower layer is a cloud layer [Eq. (11)] result in an estimated transmission loss that is approximately 27 dB too high (27 dB lower received signal). The transmission loss measurements therefore indicate that the lower layer is caused by turbulence even though cloud particles are also present.

The antenna beam positions depicted in Fig. 6 show that the beam intersections span a large horizontal distance and scattering volumes at ranges shorter than 60 km should contribute to the bistatically scattered signal. The calculations of expected transmission loss using either Eq. (11) or (12) start at the 60-km range, radar data for shorter ranges being contaminated by ground clutter. The horizontal homogeneity indicated by the nearly identical profiles A, B, and C in Fig. 4 suggests that the layers also extend to the shorter ranges not included in the computations used to generate the expected transmission loss values shown in Fig. 5. Since the computations are not for the entire scattering volume, the actual expected transmission values should be higher than those reported in Fig. 5. The local horizon in the direction of the great circle path is at an elevation angle of approximately 0.7° and is caused by coniferous trees. The tree shown on the path in Fig. 13, Ref. 4, causes a new, higher horizon of $+2.3^\circ$ but, since the tree is deciduous and was bare of leaves during the fall 1970 measurement period, should not cause shielding. The beam for the 4-foot antenna at Avon is depicted on Fig. 6 by a dot dashed line for the centerline of the pattern, the dashed lines for the upper and lower half power points, and the solid line for the 0.7° limiting horizon ray.

For the 3° Avon elevation angle and for a Westford elevation angle of 1° , the scattering volume is completely within the area used in the computations. For a Westford elevation angle of 2° , the scattering volume contained within the half power beamwidth of the Avon antenna pattern is within the area used in the computations. For the estimation of scattering by turbulence, a $[\sin(\varphi_i/2)]^{-11/3}$ factor causes scattering from the lower heights to be weighted more than scattering from higher regions. The scattering volume at distance shorter than 60 km contributes approximately the same amount to the summation in Eq. (12) as does the volume on the centerline of the transmitting beam when both the scattering angle and transmitting antenna directivity are taken into account. In the case being considered, the lower layer C_{ne}^2 value decreases rapidly with height for heights above 3 km causing the region at distances shorter than 60 km to be even more important. Assuming that the profile A in Fig. 4 represents the C_{ne}^2 values between 40 and 80 km, the 2° Westford elevation angle estimated transmission loss for turbulent scatter should be 2.5 dB higher. A similar analysis for the 2.5° Westford elevation angle indicates that the

estimated value should be 4 dB higher and for 1.5° Westford elevation angle, 0.9 dB higher. With these corrections, the expected transmission loss values for turbulent scatter are an even better match (after correction) to the measured data plotted in Fig. 5. The corrections to Eq. (11) for volumes at ranges less than 60 km and the case considered above are smaller than those listed above since the $[\sin(\varphi_i/2)]^{-11/3}$ factor is not included.

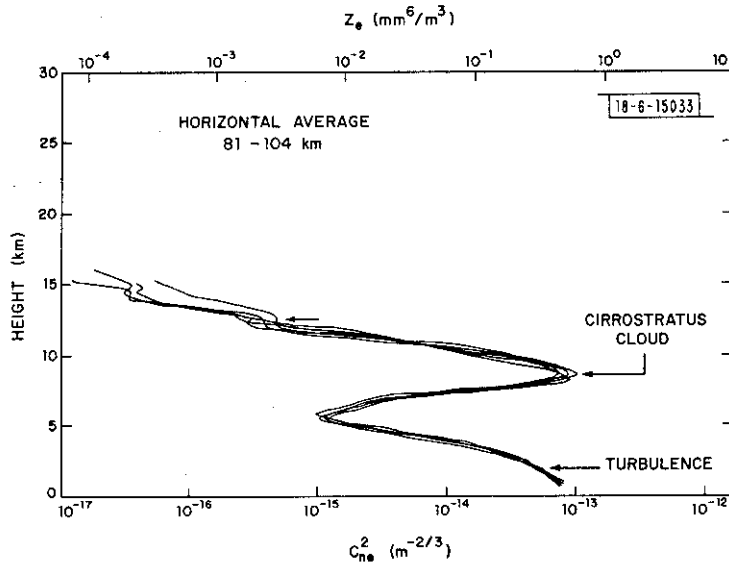


Fig. 7. C_{ne}^2 profiles, Millstone Hill radar, 229.5° azimuth, 1446-1546 and 1510-1514 GMT, 2 November 1970; Avon: 3° elevation, 49° azimuth, 4-foot antenna, vertical polarization.

The 27 dB difference between the expected transmission loss calculations based upon either the turbulence or the cloud or rain scatter assumptions (after correction as discussed above) indicates that the lower layer is caused by scattering from turbulence and not the cloud particles. Profiles for each of the elevation scans used in preparing the transmission loss estimates depicted in Fig. 5 are given in Fig. 7. Data only for the 81 to 104 km horizontal interval (A) are shown. The profile data show that little change in the intensity of the scattering layers occurred during the half hour observation period. RHI and profile data for a Westford azimuth of 230° and one hour later, 1619-1629 GMT, are shown in Figs. 8 and 9. The RHI display shows an upper cirrostratus layer and an intensified lower layer. Interval B below 4 km is blank indicating Z_e values greater than 0 dBZ. A peak Z_e value of 25 dBZ was detected at a height between 2 and 3 km at a range of 120 km. The peak Z_e value was in the melting layer (just below the height of the 0°C isotherm) and corresponds to the transition from snow above to very light rain below. The profiles depicted in Fig. 9 for the same elevation scan show that the cirrostratus layer changed in intensity by only a few dB and the thickness and intensity of the lower layer increased from the earlier values shown in Figs. 4 and 7. The data used in generating the profile are only the data displayed on Fig. 8, the blank area corresponding to snow and rain was excluded from the horizontal averaging.

The estimated and measured transmission loss data are shown in Fig. 10. Computations based upon both the turbulence and the cloud or hydrometeor particle scatter models are shown. For elevation angles greater than 4° only the cloud model is pictured, the turbulence model not being appropriate for the upper layer. For elevation angles below 2.5°, the turbulence model

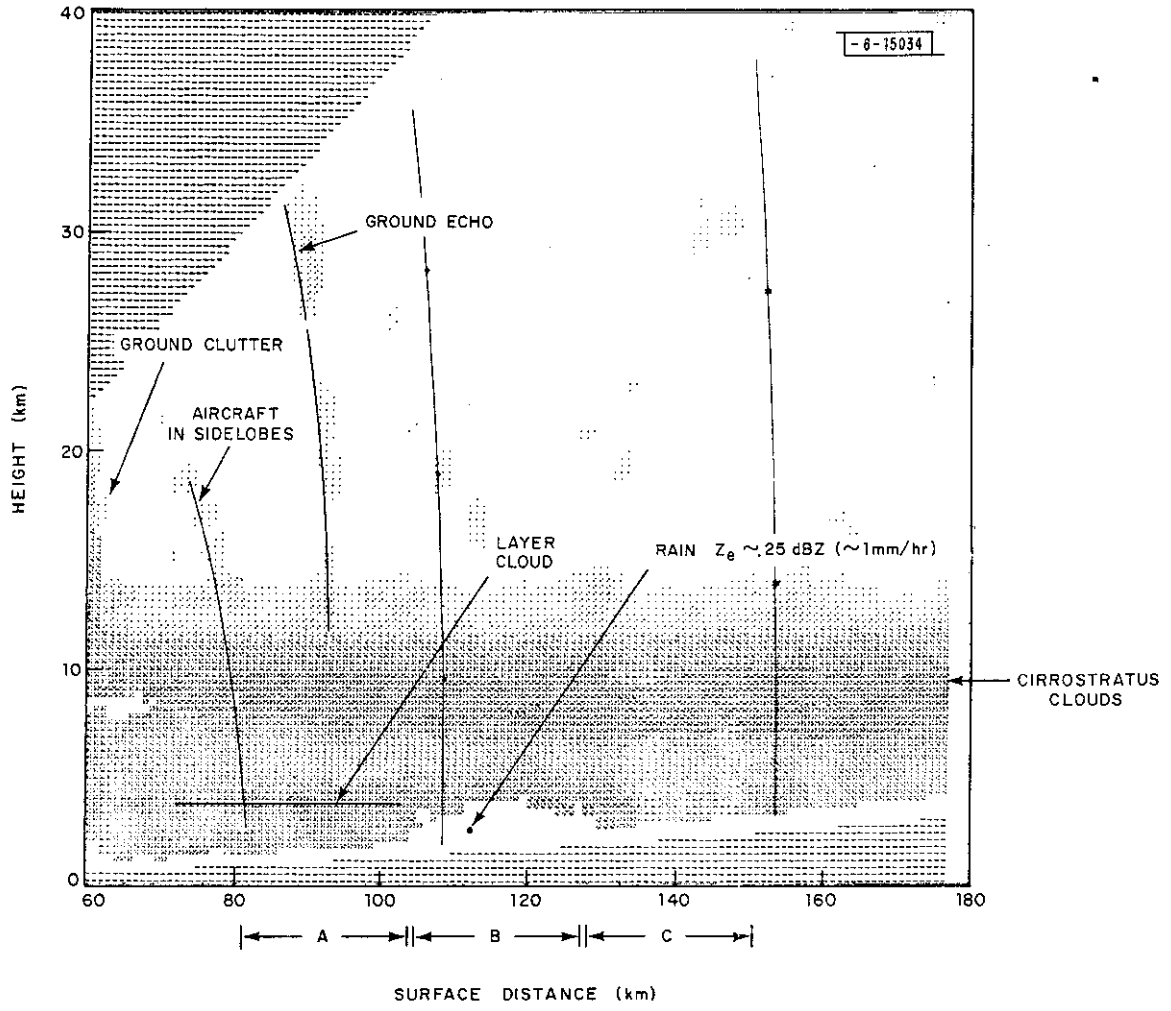


Fig. 8. RHI display, Millstone Hill radar, 230° azimuth, 1619-1626 GMT, 2 November 1970.

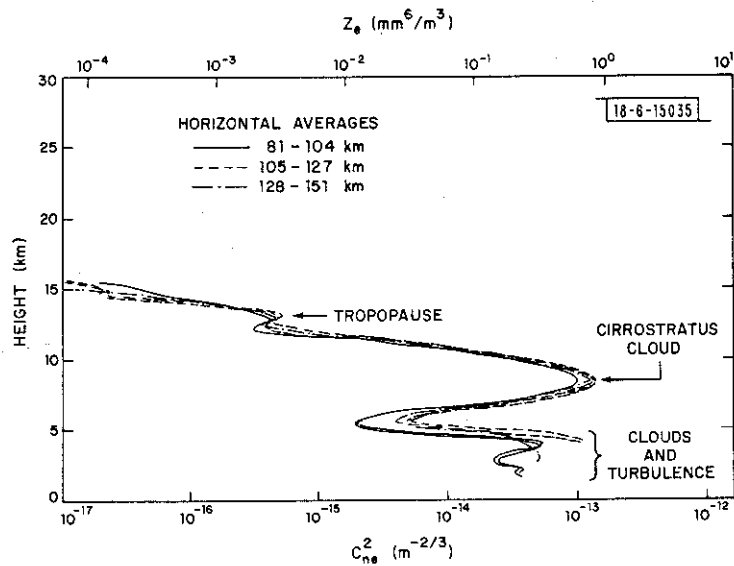


Fig. 9. C_{ne}^2 profiles, Millstone Hill radar, 230° azimuth, 1619-1626 GMT, 2 November 1970; Avon: 6° elevation, 49° azimuth, 4-foot antenna, vertical polarization.

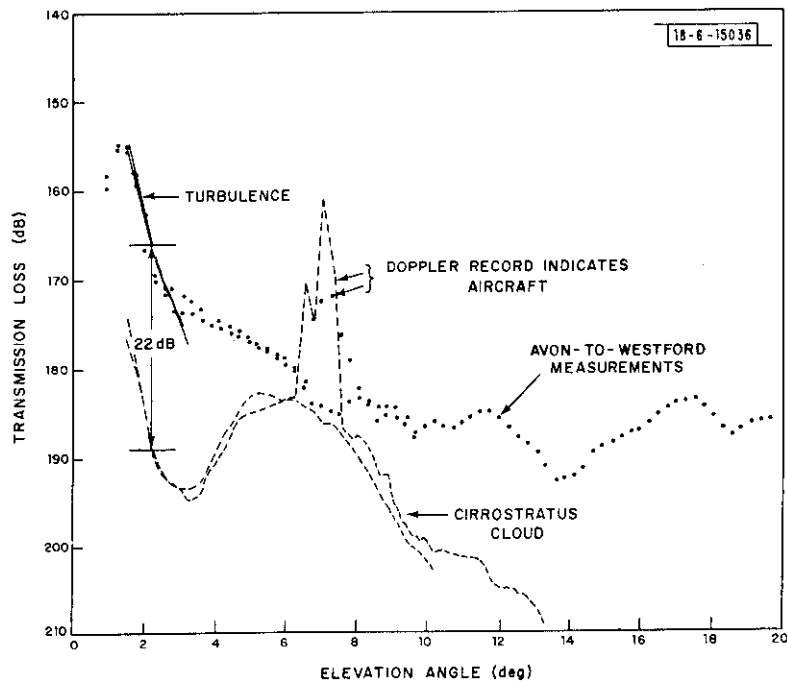


Fig. 10. Calculated and measured transmission loss, Avon-to-Westford scatter path, 230° azimuth (Westford), 1619-1626 GMT, 2 November 1970; Avon: 6° elevation, 49° azimuth, 4-foot antenna, vertical polarization.

appears to provide a good fit to the measurements. The cloud or hydrometeor model computations underestimate the measured data by 22 dB. For the scans depicted in Fig. 10, the Avon antenna was elevated at 6°. For Westford elevation angles below 3°, the contribution to the received signal from scattering volumes at distances less than 60 km from Westford is small (less than 1.0 dB) even for the turbulence model because the Avon antenna directivity is more than 20 dB lower in the direction of the neglected scattering volumes than in the direction of the centerline of the antenna pattern. The primary contribution to the scattering observed below 2.5° is either from snow and at a 1° elevation angle from melting snow in the bright band observed at ±20 km from Westford for the cloud or hydrometeor model or from turbulence at 70 to 80 km from Westford for the turbulent model. Dennis¹⁰ in earlier observations of forward scatter from the bright band measured signal levels 6 to 15 dB higher than predicted using Rayleigh scattering theory. A 22-dB enhancement due to an increase in the forward scatter cross section per unit volume for snow and melting snow would bring the cloud and hydrometeor scatter computations into agreement with the measurements at Westford elevation angles below 2.5° but seems to be a rather large correction to assume.

Although the turbulence model fits the measurements, the increased C_{ne}^2 values reported for the lower layer are not consistent with the earlier C_{ne}^2 values and the observations of increased cloudiness and rain at the lower levels suggest that scattering from the snow may contribute in part to the measured data. Additional support for the turbulent origin of the observed low elevation angle data, however, is provided by the Doppler shift measurements. Figure 11 shows the Doppler shift to be -2 to -4 Hz at elevation angles below 2.0°. Similar data taken one hour earlier showed the Doppler shifts to be between +0 and -1 Hz for scattering by turbulence. The difference between the great circle path and 230° azimuth Doppler data is in the order of -1 to -3 Hz.

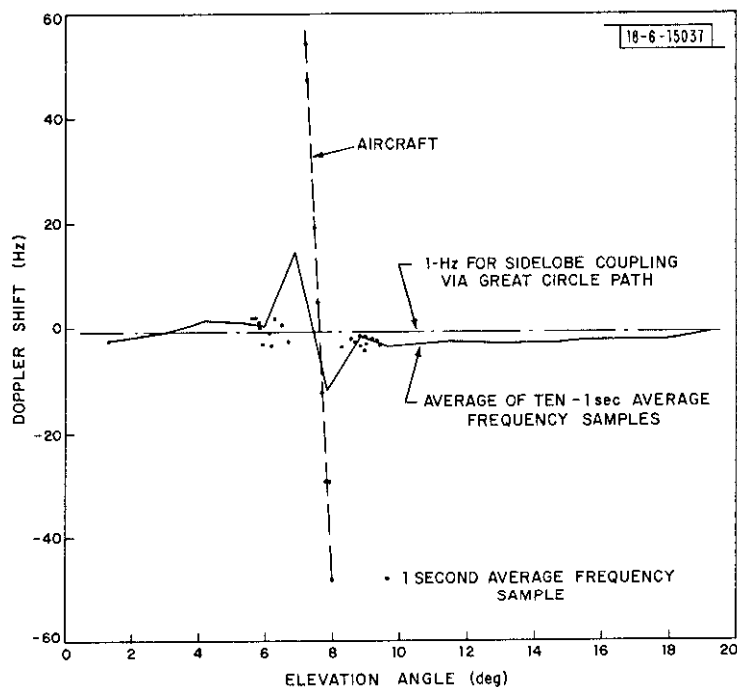


Fig. 11. Doppler shift measurements, Avon-to-Westford scatter path, 230° azimuth (Westford), 1622-1626 GMT, 2 November 1970; Avon: 6° elevation, 49° azimuth, 4-foot-horn antenna.

The computed Doppler shift due to horizontal winds measured by a radiosonde flight two hours later is between 0 and -1 Hz for scattering either at 80 km (turbulence) or 120 km (snow) from Westford. Snow, however, typically has a fall velocity of 1 to 2 m/sec which would cause the Doppler shift to be between $+2$ and $+5$ Hz for the 120 km scattering location. Since the Doppler data do not agree with the snow scattering hypothesis, turbulence was responsible for the measured signals.

The Doppler data also show a perturbation caused by scattering from an aircraft. When the signal from the moving aircraft is large in comparison with the other signals, the phase lock loop tracks the aircraft Doppler shift as shown. The Doppler signature of the aircraft was used to eliminate the measured and computed transmission loss values for elevation angles between 6° and 8° from further analysis. The measured data displayed both on Figs. 5 and 10 show generally smaller measured transmission loss values (larger received signal) than those estimated by either mode of computation for elevation angles above 4.0° . This is caused by sidelobe coupling into the Westford antenna from either the generally high level great circle path signal or, on rare occasions, high signal levels due to scatter from precipitation. The sidelobe coupled signals may generally be identified by the lack of change of the reported Doppler shift with antenna position. In the data analysis, all signals that are identified as arising from sidelobe coupling (into the Westford antenna) were deleted. This was generally done by deleting all signals more than 17 dB below the largest signal observed in a set of scans.

Data for scattering from the cirrostratus cloud are shown in Figs. 12 and 13. Figure 12 shows the RHI display for an azimuth angle in the set of azimuth scans given in Fig. 13. The cirrostratus layer had increased in intensity in comparison with the earlier data reported above and had a peak value of 15 dBZ. The layer was horizontally homogeneous over a rather large area. Beyond 115 km, rain and snow are indicated, the hydrometeor type depending upon height. In the melting layer, Z_e values between 35 and 40 dBZ were observed. The snow was at sufficient distance from Westford that it was not observed bistatically except at a height within the cirrostratus layer. The RHI shows an extensive region beyond 130 km and above 15 km with Z_e values greater than -30 dBZ. These data were caused by rain and snow near the surface as detected through the sidelobes of the Millstone Hill L-band antenna.

The transmission loss computations given in Fig. 13 are for scattering by cloud particles. Except for elevation angles below 3° on the 200° azimuth scan, the calculations do not change with azimuth. The lack of change with azimuth is due to the horizontal homogeneity of the cirrostratus layer for distances from Westford less than 100 km, the nearly uniform illumination of the scattering layer by the standard gain horn, and the small variation in ρ_i [see Eq. (11)]. The measurements displayed in Fig. 13, however, show a progressive change in transmission loss with azimuth for elevation angles below 4° . Above this elevation angle, the measured and estimated transmission loss values differ by 7 to 8 dB. The increase in transmission loss with decreasing azimuth value for a fixed value of elevation angle is caused by shielding by the local horizon at Avon. The computations were made using a 0.7° horizon elevation angle depicted by the dashed curve on Fig. 1. The distant horizon indicated in Fig. 13, Ref. 4 for Avon azimuth angles between 70° and 90° varies from 2.4° to 2.6° elevation and, at these elevation angles, Fig. 1 indicates that for a Westford elevation angle of 1.5° , the layer should not be illuminated for Westford azimuths less than 210° . The deciduous tree in the near horizon did not cause shielding because it was bare of leaves. For a Westford elevation angle of 2° , the layer should be visible at 100 km at a Westford azimuth of 200° but not visible at that range at an azimuth of

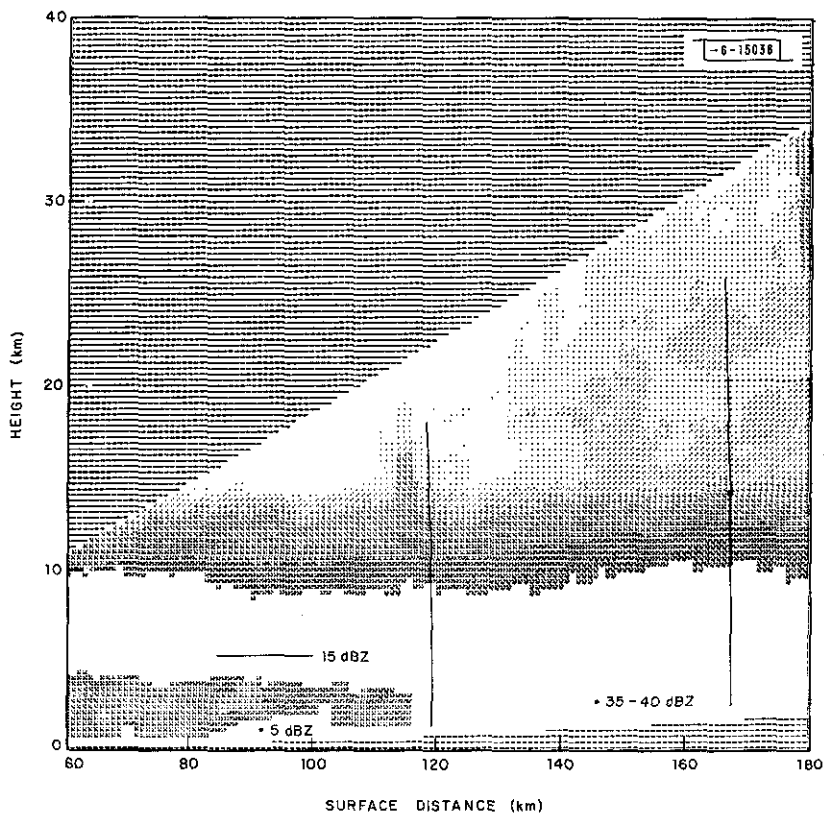


Fig. 12. RHI display, Millstone Hill radar, 195° azimuth, 1954-1957 GMT, 2 November 1970.

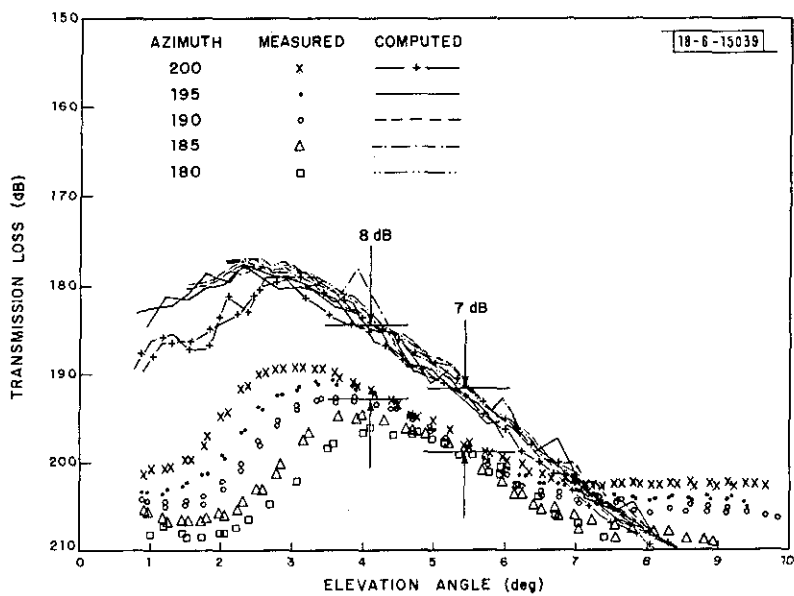


Fig. 13. Calculated and measured transmission loss, Avon-to-Westford scatter path, 200-180° azimuth (Westford), 1951-2008 GMT, 2 November 1970; Avon: 10° elevation, 70° azimuth, horn antenna, vertical polarization.

190°. The measurements at 200° azimuth differ from the estimated values by 13 dB and 9 dB for a Westford elevation angle of 1.5° and 2°, respectively. The difference obtained at an elevation angle of 2° is within a dB or two of the difference observed between elevation angles of 4° and 5° where no shielding or obstruction of the transmit beam occurs. The difference at 2°, for 190° azimuth direction, is the same as the difference for a 1.5° elevation angle at 190° azimuth direction and is greater than 20 dB. The data therefore show shielding by the horizon to be effective at 190° azimuth angle and much less effective at 200° azimuth.

Scattering due to snow is depicted in Figs. 14 and 15. The RHI display presented in Fig. 14 is different from the displays presented above because only Z_e values above 0 dBZ are displayed. Each dot on this display represents 5 dB above the 0 dBZ threshold. The highest Z_e value on the display, 45 dBZ, occurs in the melting layer at 85 km range and 1.5-1.7° Westford elevation angle. Higher elevation angle data are for scattering by snow. The computations shown in Fig. 15 are for a 0.7° shielding elevation angle (local horizon) at Avon. Above a 2.0° Westford elevation angle and distances between 80 and 100 km from Westford, the snow scatterers have clear lines-of-sight both to the transmitter and to the receiver. For the snow scatterers with clear lines-of-sight the measured transmission loss is 4 dB greater than the calculated values (the received signal was 4 dB lower than calculated). Above 4° Westford elevation angle the difference between the measured and computed transmission loss values is due to sidelobe coupling (Westford antenna sidelobes).

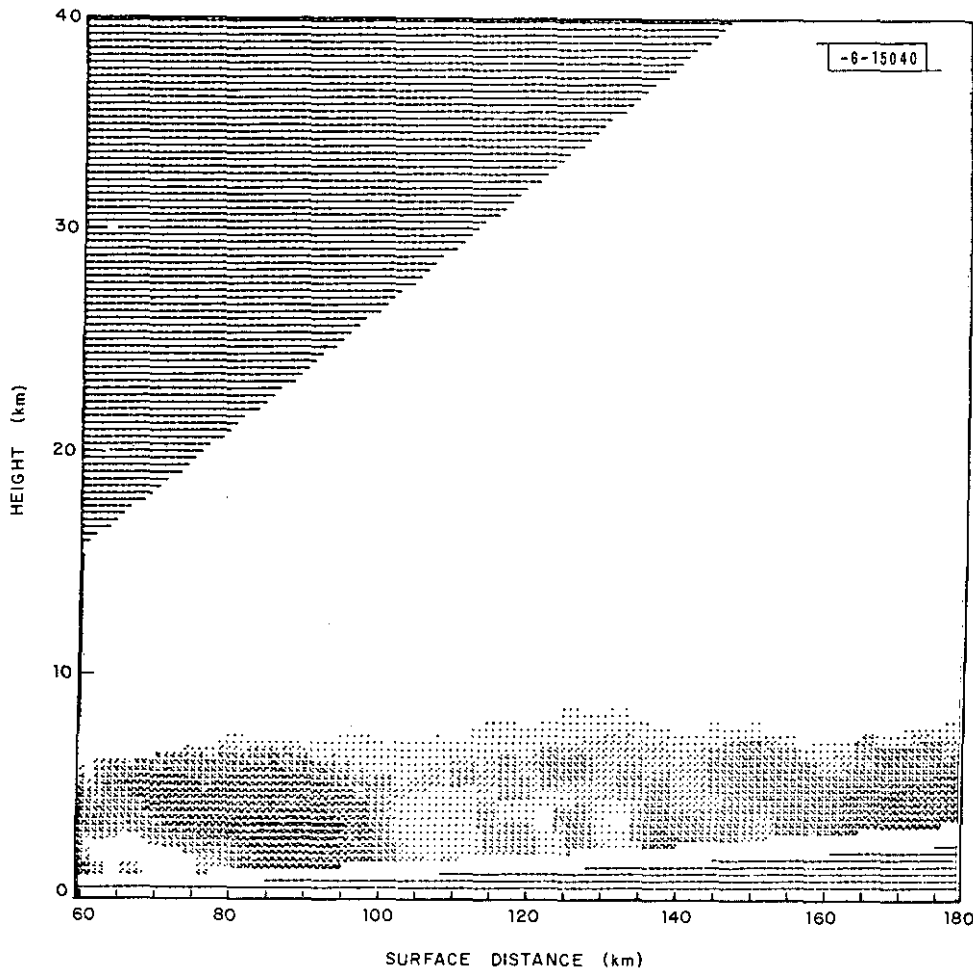


Fig. 14. RHI display, Millstone Hill radar, 216° azimuth, 1750-1753 GMT, 13 November 1970.

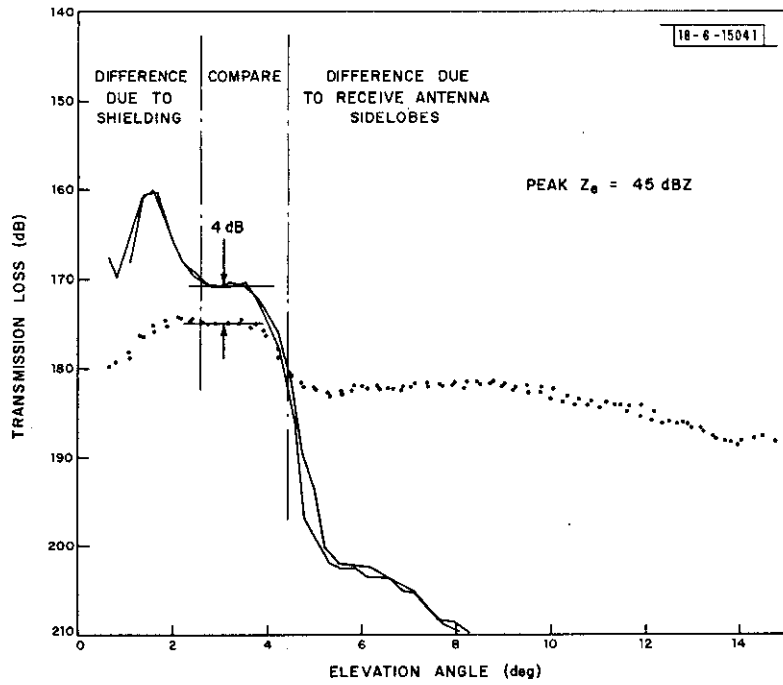


Fig. 15. Calculated and measured transmission loss, Avon-to-Westford scatter path, 216° azimuth (Westford), 1750-1756 GMT, 13 November 1970; Avon: 10° elevation, 49° azimuth, horn antenna, vertical polarization.

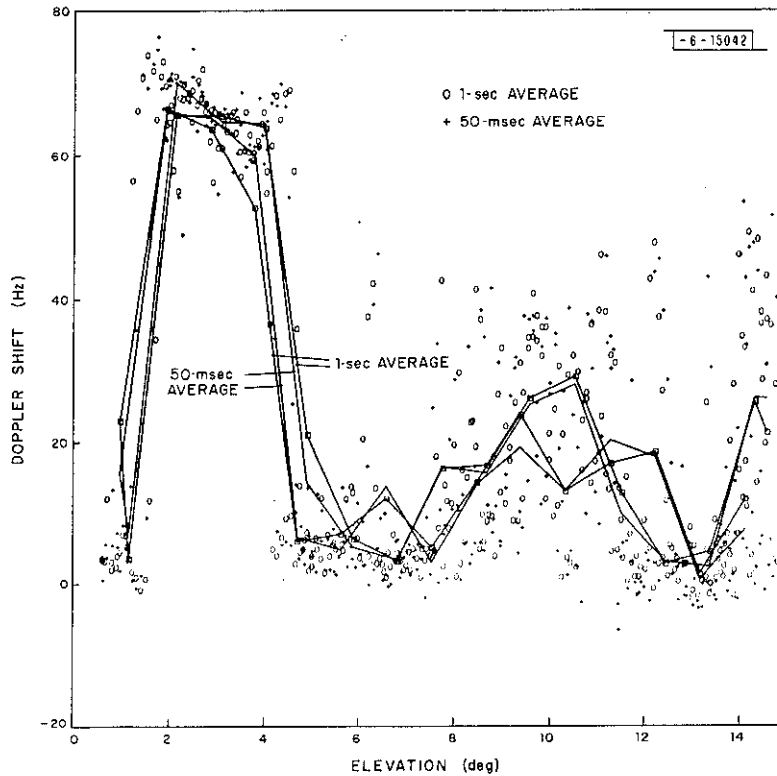


Fig. 16. Doppler shift measurements, Avon-to-Westford scatter path, 216° azimuth (Westford) 1750-1756 GMT, 13 November 1970.

Evidence for the sidelobe coupling is given by the Doppler data in Fig. 16. Between 2° and 4° Westford elevation angle, the Doppler shift is between +60 and +70 Hz. For snow at 2° elevation angle and 100 km from Westford, an expected Doppler shift of +70.4 Hz was computed using Eq. (5) of Ref. 5, radiosonde data obtained during a flight launched at 1755 GMT while the measurements were being taken, and an assumed 1 m/sec fall velocity for the snow. The measured Doppler shift values for a 2° elevation angle are within 1 Hz of the estimated value. The Doppler data show that scattering by snow was observed for Westford elevation angles between 2° and 4°. Above 4°, the Doppler data are approximately 0 Hz and above 6° oscillate between 0 Hz and +50 Hz. The 0 Hz data is indicative of sidelobe coupling along the great circle path. The oscillatory data indicate the phase lock loop is hunting, oscillating between the snow scatter signals and the great circle path signal. The 0 Hz data for Westford elevation angles less than 1.5° indicate that the data are for great circle path propagation and not snow scatter.

The melting layer observed in the calculated transmission loss values is not evident in the measured data. The Doppler data indicate that no signals were obtained from the vicinity of the melting layer for Westford elevation angles below 1.5°. The line-of-sight from Avon to the scattering volumes along the Westford antenna beam for a 2° Westford elevation angle and ranges between 80 and 100 km have Avon elevation angles ranging from 2.3° to 2.5° and Avon azimuth angles ranging from 65° to 76°. Over this azimuth range, Fig. 13, Ref. 4 shows a deciduous tree with horizon angles above 4° and the distant horizon (also trees) at elevation angles between 2.2° and 2.4°. During the fall measurement period the near tree was bare of leaves. Some of the trees on the distant horizon were bare of leaves and some were conifers. The many distant trees still provided a distinct horizon as shown in Fig. 13, Ref. 4 and discussed above. Below a Westford elevation angle of 2°, the lines-of-sight from the Avon antenna to the scattering volume are obstructed and site shielding occurs. Figure 15 indicates that more than 10 dB of shielding was obtained.

The measurements made during the fall 1970 period were elevation scans with Avon site shielding evident at low elevation angles and sidelobe coupling evident at high angles. From an examination of each of the elevation scans together with the simultaneously obtained Doppler data, 38 elevation scans were identified that had measurements of scattering from snow with unobstructed lines-of-sight. A histogram of the ratios of the measured-to-calculated transmission loss values (differences in dB) is shown in Fig. 17.

Measurements of scattering from turbulent layers at Westford elevation angles below 2.5° and Westford azimuth angles within 2.5° of the great circle path were compared with computations for data taken between 1446 and 1626 GMT on 2 November 1970. Several of the elevation scans used in the comparison were discussed above. Data for 164 separate 6-second average measurements from 15 elevation scans were used to generate the histogram given in Fig. 18.

B. Summer 1970

During the summer of 1970 data were acquired using azimuth scans. Both the Millstone Hill L-band radar and the Westford 60-foot antenna were scanned so both antennas were pointed in the same direction at the same time. The simultaneous azimuth scan measurement mode was used only when rain was detected somewhere in the surveillance area common to both the radar and bistatic scatter system. Measurements of scattering by turbulence were conducted using elevation scans as described in the previous section. During the summer measurement program the radar and bistatic scatter system were not scanned to observe the same volume when observing scatter from turbulence.

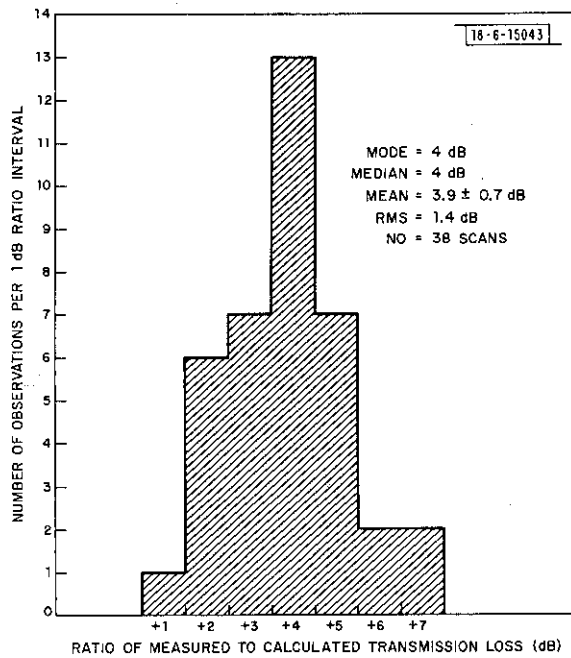
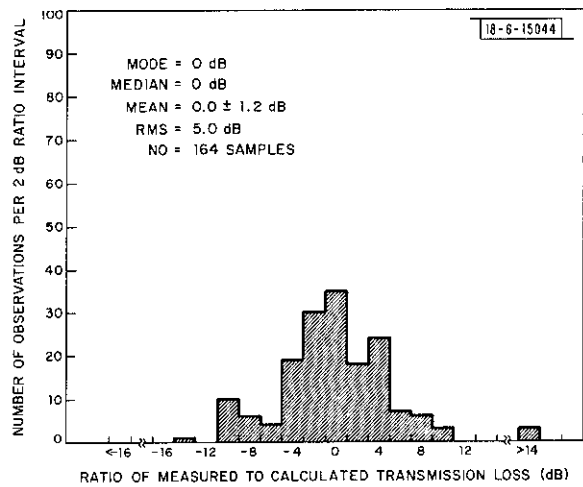


Fig. 17. Histogram of ratios of measured-to-calculated transmission loss, snow, fall 1970 C-band data.

Fig. 18. Histogram of ratios of measured-to-calculated transmission loss, turbulence, fall 1970 C-band data.



The weather on the 10 measurement days between 20 and 31 July 1970 varied from clear to showery. Rain data from the three showery days, 28, 29, and 30 July were processed for comparison between measured and computed transmission loss. During the showery days, the 0° isotherm varied in height from 4.1 to 4.3 km. The measurements spanned a range of Z_e values from 20 to 55 dBZ and a range of heights from 2 to 9 km. The hydrometeor types sampled were rain, snow, and melting snow.

A preliminary description of the summer measurements including a detailed presentation of the computer output for an azimuth scan is given in Section V of Ref. 4. The azimuth scan given in Ref. 4 was obtained between 0209 and 0220 GMT on 29 July 1970. The comparison between measured and computed transmission loss values is presented in Fig. 23 of Ref. 4 and shows the average of the logarithm of the ratio of measured-to-calculated transmission loss values to be 0.6 dB. The azimuth scan, although showing good agreement between measurement and calculation, was not typical of measurements made during the summer observation period. The rain cells that contributed to the observed scattered signal were within the area for clear lines-of-sight from the transmitter to scattering volume to receiver bounded by the heavy solid and dot dashed lines on Fig. 1. The cells, however, were not within the main lobe of the transmitting horn antenna pattern and some measurement error due to gain uncertainty (due to antenna pointing and the difficulty of making accurate sidelobe directivity measurements) was possible.

A section of a computer generated plan position indicator (PPI) display is shown in Fig. 19. Although several rain cells and rain cells imbedded in a larger mesoscale rain area (top of the PPI section) are shown, only those in the area marked clear lines-of-sight were useful for comparison. The other cells may still be detected bistatically but at reduced signal levels due to the obstacles. At higher elevation angles, the clear lines-of-sight area enlarges increasing the number of possible locations for useful rain scatter analysis. A series of azimuth scans displaying bistatic scatter system transmission loss measurements is shown in Fig. 20 together with the Doppler shift data for each of the measurements. The successive scans show that the cells at Westford azimuth angles less than 270° were either dissipating or changing Z_e value with height because the transmission loss increased with height or elevation angle and the cells were within clear lines-of-sight area. The cell at an azimuth angle 280° was bistatically detected at an elevation angle 1.5° but the received signal was not as strong as for Westford elevation angles above 2° . At the higher elevation angles the cell was within a clear lines-of-sight area. The Doppler data show that for Westford elevation angles above 1° the Doppler shift continued to increase with increasing azimuth angle indicating that hydrometeor scattering was being detected but at a reduced level. The abrupt changes in Doppler shift at 280° azimuth are due to the local changes in the wind field near the cell. The measured and calculated transmission loss values for the 1.5° elevation angle scan depicted in Fig. 19 are given in Fig. 21. The effect of site shielding is indicated by the two curves, one computed using the table of local horizon elevation angles for the Avon site and the other computed using a 0.7° horizon angle. In the data processing, transmission loss values were accepted for use in generating the comparison histograms when the computations with shielding (using the local horizon value table) and without shielding (using the 0.7° value) were identical. The abrupt loss of radar data between 253° and 256° azimuth was due to a radar system malfunction, bistatic data were observed in this region as shown by the data.

Two comparison histograms were prepared for the summer 1970 data. The first histogram is given in Fig. 22 and is for rain cells within the clear lines-of-sight area and within the 10 dB down points on the transmitting antenna directivity [$g_2(\hat{\rho}_1)$] pattern. The

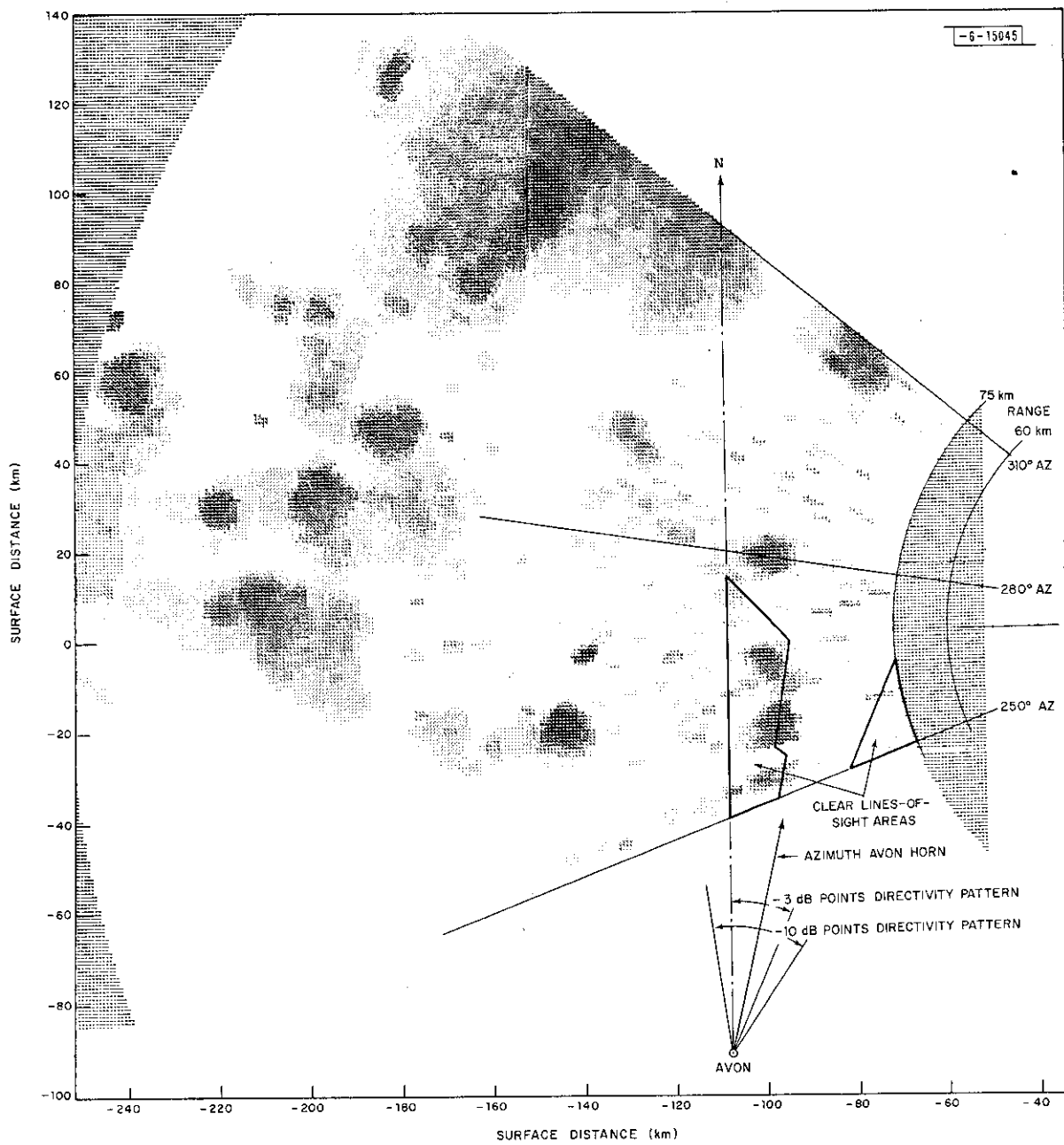


Fig. 19. PPI display, Millstone Hill radar, 1.5° elevation, 2046-2056 GMT, 28 July 1970.

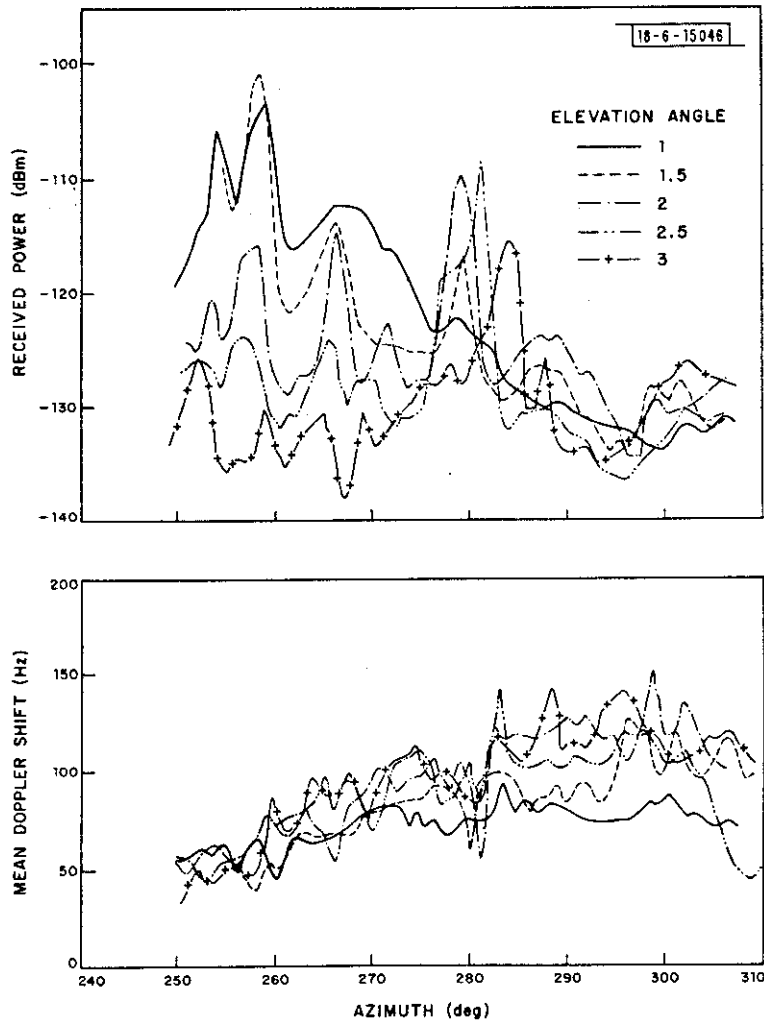


Fig. 20. Measured transmission loss and Doppler shifts, Avon-to-Westford scatter path, 1.0 to 3.0° elevation (Westford), 2046-2132 GMT, 28 July 1970.

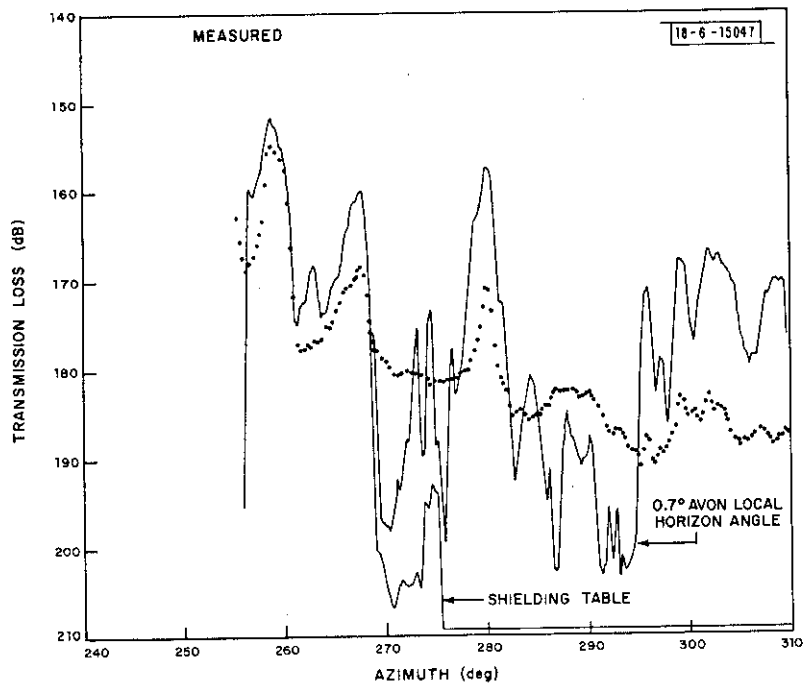


Fig. 21. Calculated and measured transmission loss, Avon-to-Westford scatter path, 1.5° elevation (Westford), 2046-2056 GMT, 28 July 1970.

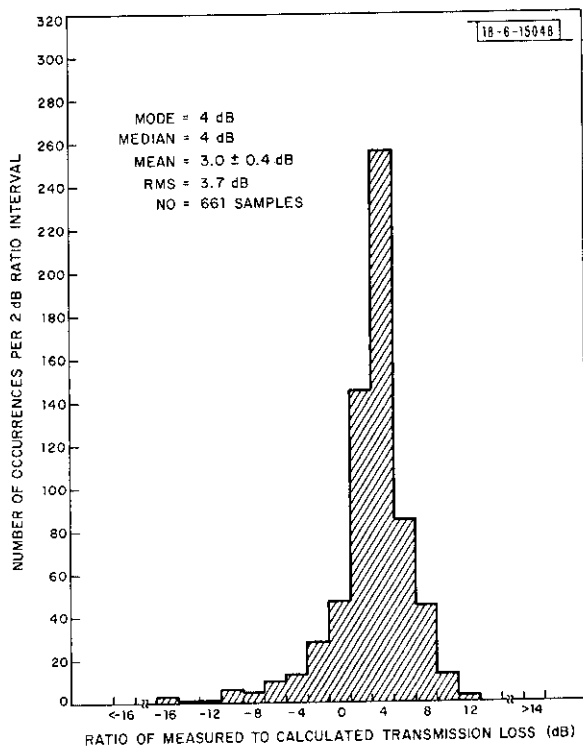


Fig. 22. Histogram of ratios of measured-to-calculated transmission loss, rain within clear lines-of-sight and -10 dB Avon antenna pattern function, summer 1970, C-band.

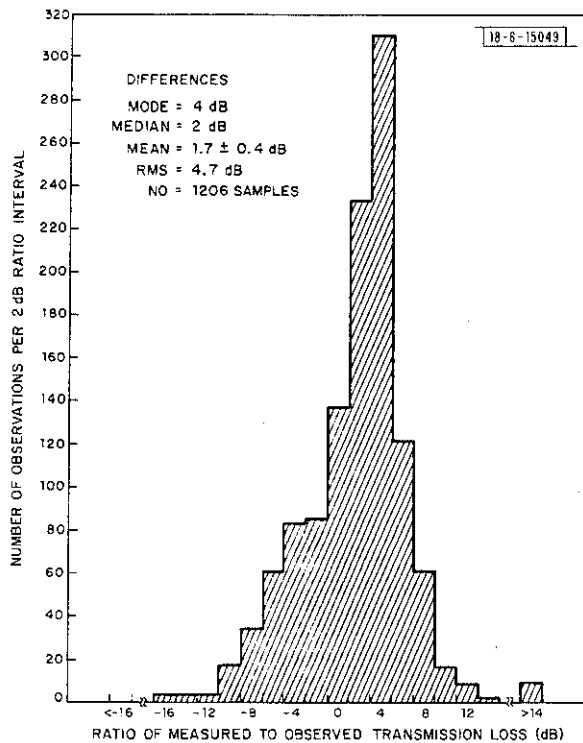


Fig. 23. Histogram of ratios of measured-to-calculated transmission loss, rain with clear lines-of-sight, summer 1970, C-band.

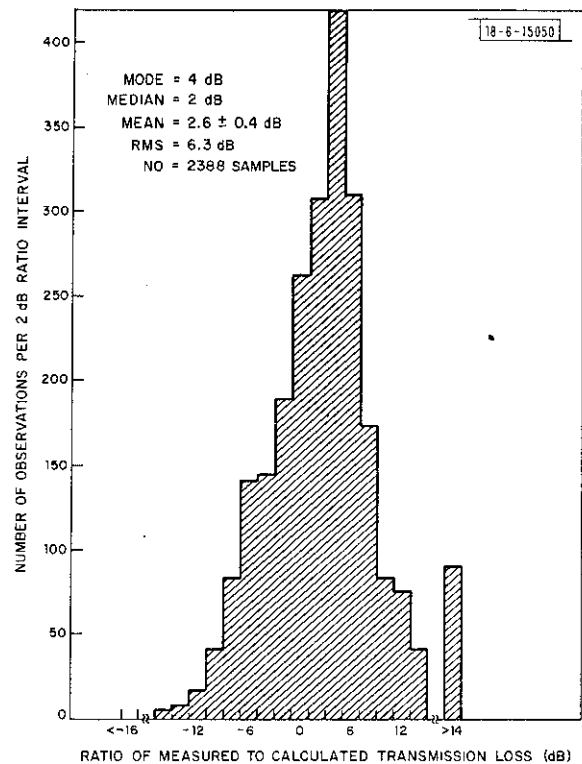


Fig. 24. Histogram of ratios of measured-to-calculated transmission loss, all rain data prior to culling, summer 1970, C-band.

second histogram is for all cells within the clear lines-of-sight area and is presented in Fig. 23. In constructing the histograms, the 17-dB threshold described in Section V, Ref. 4 and an additional -17-dB threshold with respect to the peak received bistatically scattered signal for a set of scans were used to further screen the data. An additional histogram was generated for all observations using the 0.7° local horizon (no shielding) and is presented in Fig. 24. This last histogram displays the raw data prior to culling (the 17-dB threshold discussed in Ref. 4 was used to remove cases of sidelobe coupling).

C. Summer 1968

During the summer of 1968, data were acquired using azimuth scans. The radar system used for the 1968 measurements was the same as used in 1970 with the exception of using only one receiver thereby limiting the dynamic range to 40 dB. The effective system dynamic range was increased by manually varying the attenuator between the antenna and receivers between scans. The bistatic scatter system was different from the 1970 system because a higher frequency, 7.74 GHz, was used and the transmitting and receiving antenna polarizations were horizontal and left-hand circular, respectively, rather than vertical and vertical.

The weather on the 10 measurement days between 29 July and 9 August 1968 varied from clear to showery. Showers occurred on four of the days, August 2, 6, 7, and 9. The transmitting antenna used on 2 August was the 6-foot antenna and insufficient data with comparisons for rain cells within the -10 dB points on the antenna directivity pattern were obtained for analysis. During

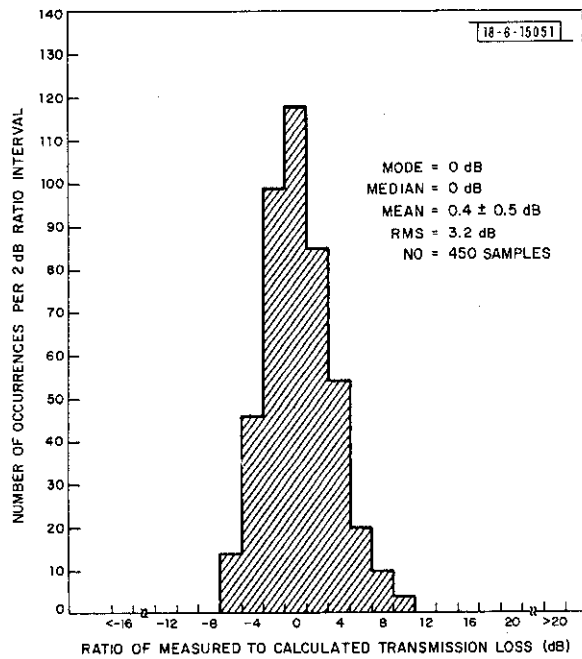


Fig. 25. Histogram of ratios of measured-to-calculated transmission loss, rain within clear lines-of-sight and -10 dB Avon antenna pattern function, summer 1968, X-band.

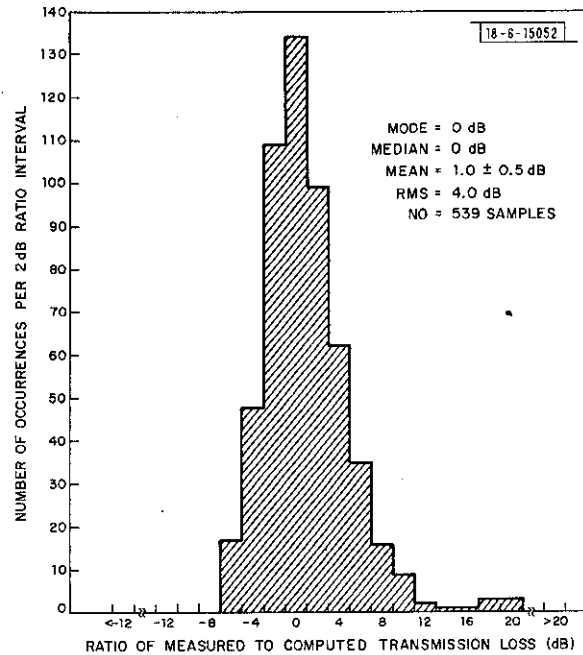


Fig. 26. Histogram of ratios of measured-to-computed transmission loss, rain within clear lines-of-sight, summer 1968, X-band.

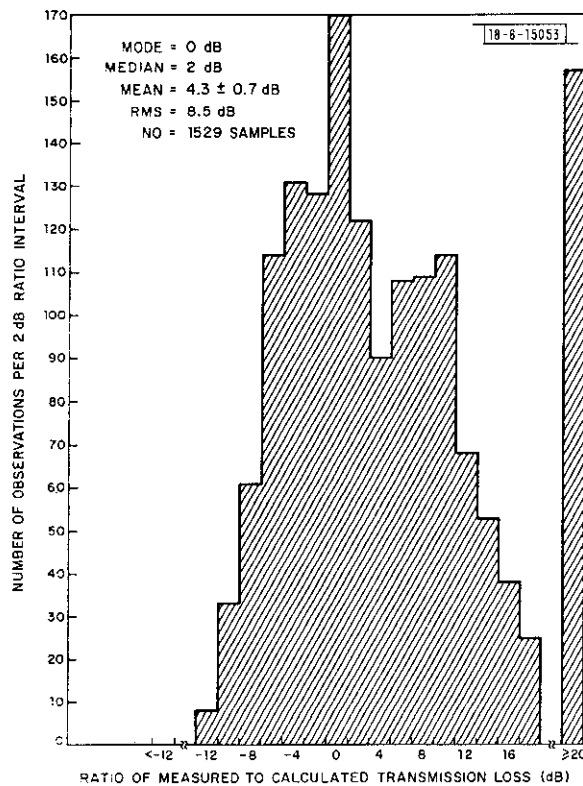


Fig. 27. Histograms of ratios of measured-to-calculated transmission loss, all rain data prior to culling, summer 1970, X-band.

the latter three days, the standard gain horn was used for transmitting at Avon and data were obtained and processed for these days.

A preliminary analysis of data from the summer 1968 measurements is given in Ref. 3. The azimuth scan data given in Figs. 8, 9, and 10 of Ref. 3 are similar to the data presented above with site shielding effects in evidence. The analysis performed in Ref. 3 assumed that the circularly polarized receiving antenna detected one half the energy that would be detected by a horizontally polarized antenna. The M_1 factor discussed in Section III and used in the present analysis includes scattering due to both the horizontal and vertical polarization components of the incident field present at the scatterer and caused by the geometry of the scattering problem. The difference between the present analysis and that reported in Ref. 3 is small except for scattering angles near 90° (see Fig. 2).

The data were culled prior to the construction of histograms comparing the measured and computed values using the methods described above. The histogram for all data within the clear lines-of-sight area and the -10 -dB points on the transmitting antenna pattern is given in Fig. 25 and the histogram for all data within the clear lines-of-sight area and any directivity value is given in Fig. 26. The histogram for data prior to culling for inclusion in the clear lines-of-sight area is given in Fig. 27.

V. ANALYSIS OF DATA

A. Best Estimate Comparison

The transmission loss measurements made during each of the three phases of the Avon-to-Westford were compared with calculations made using the appropriate approximate description of scattering by either hydrometeors (or cloud particles) or turbulence. The comparisons are presented as histograms of the logarithm of the ratio of measured-to-calculated transmission loss (expressed in dB). The comparison histograms are characterized by their mode, median, mean, and rms variation values in Table V. The comparisons were made using the data as provided by the computer program and the equations described in Section 3 and in Ref. 4. The ratio (difference in dB) for the most accurate computations for each measurement period are $+3.0$ dB for hydrometeors, summer of 1970; $+3.9$ dB for snow, fall of 1970; $+0.4$ dB for hydrometeors, summer of 1968; and 0.0 dB for turbulence, fall of 1970. The maximum uncertainty in these ratios due to equipment calibration error (neglecting the items mentioned above) is 2.7 dB for 1970 and 3.7 dB for the summer of 1968 (Table IV above). The 1970 rain data show differences between the measured and computed transmission loss values that are larger than the measurement and computational uncertainties listed in Table IV.

One source of equipment-caused error noted in Ref. 4 was the possible Westford receiver calibration error. These errors were less than 0.5 dB for any set of scans and vary from set to set. On average, for a number of sets of scans, these errors vary about a zero mean (the errors shown for 29 July 1970, Fig. 10, Ref. 4 are $+0.2$ and -0.3). The calibration errors contribute only to the repeatability values which in turn contribute to the rms variation in the ratios of measured-to-computed transmission loss (see Table II, Ref. 4). The second source of possible equipment-caused error that was not corrected for in the computer program was the effect of post detection averaging by the 50 Hz filter in the AGC loop. If the correlation time for the scattering process is long in comparison with the approximate 20 msec averaging time of the post detection filter, the filter passes the received signal without integration and the output of the computer program is correct. If the correlation time is short in comparison with 20 msec,

TABLE V
SUMMARY OF COMPARISON HISTOGRAMS

	Compare	Mode (dB)	Median (dB)	Mean* (dB)	RMS (dB)	No. of Samples
C-band Rain – Summer 1970 within clear lines-of-sight and –10 dB	6-sec avg.	+4	+4	+3.0 ± 0.4	3.7	661
C-band Rain – Summer 1970 within clear lines-of-sight	6-sec avg.	+4	+2	+1.7 ± 0.4	4.7	1206
C-band Rain – Summer 1970 all data above 0.7° Avon horizon angle	6-sec avg.	+4	+2	+2.6 ± 0.4	6.3	2388
X-band Rain – Summer 1968 within clear lines-of-sight and –10 dB	6-sec avg.	0	0	+0.4 ± 0.5	3.2	450
X-band Rain – Summer 1958 within clear lines-of-sight	6-sec avg.	0	0	+1.0 ± 0.5	4.0	539
X-band Rain – Summer 1968 all data above 0.7° Avon horizon angle	6-sec avg.	0	+2	4.3 ± 0.7	8.5	1529
Fall 1970 C-band Turbulence	6-sec avg.	0	0	0.0 ± 1.2	5.0	164
Fall 1970 C-band Snow	scan	+4	+4	3.9 ± 0.7	1.4	38

* Range of possible values is $\pm 3\sigma$.

the filter passes the average amplitude of the signal and a 1.05-dB (not 1.14-dB as quoted in Ref. 4) correction is required. The correction is for the relationship between the average of the amplitude and the average of the square of the amplitude for a stationary Rayleigh process.¹¹

The correlation time for the scattered signal is the inverse of the Doppler spread. The Doppler spread may be estimated for the different locations of the scattering volume using the equations presented in Ref. 5. For scattering from positions within a few degrees (at Westford) of the great circle path, the Doppler spread is less than 1 Hz for scattering by turbulence and 10 to 20 Hz for scattering from rain for either the C- or X-band measurements. Near great circle path measurements therefore do not require correction. For off great circle path scattering, the Doppler spread due to turbulence and changes in hydrometeor fall velocity ranges from 20 to 40 Hz for C-band and is nearly twice these values at X-band. The Doppler spread due to the wind shear may be considerably larger;⁵ typically being 100 Hz or more at C-band. Due to the large values of wind shear possible in the showery rain observations, the 1.05-dB correction should be applied. Occasionally the Doppler spread was checked at the Westford site and on one occasion a spread of greater than 500 Hz (10-dB down points) was observed during the summer of 1968. Because of the large possible Doppler spreads, the 2880 Hz IF bandwidth filter system was generally used for rain measurements during 1970. The 1-dB increase in calculated transmission loss required to correct for Doppler spread moves the C-band data into closer agreement for hydrometeor scatter but causes a larger disagreement in the X-band comparisons.

The bistatic scatter paths must be longer than 143 km, the surface distance between the transmitter and receiver and may be as long as 200 km and be within the clear lines-of-sight area. These paths reach to heights between 2 and 9 km and are subject to a small amount of attenuation due to gaseous absorption. Computations of the specific attenuation for gaseous absorption show a value of approximately 0.01 dB/km at the surface and 0.002 dB/km at 7-km height at 4.5 GHz for the measurement periods used. Using an effective ray height of 2 km, the specific attenuation is approximately 0.006 dB/km and the total attenuation along the path should vary from 0.9 to 1.2 dB. Choosing a value of 1.0 dB as typical for the scattering paths used, at C-band an additional 1.0-dB transmission loss increase is required to correct the C-band computations for gaseous absorption along the path. The L-band radar data are also subject to attenuation due to oxygen absorption. The attenuation at L-band is approximately 0.6 dB (2 way) for a scatterer at 100 km and, after subtracting 0.4 dB for the effect of oxygen absorption on the measurement of the radar antenna gain (gain is in error by 0.2 dB), the radar cross section estimates are approximately 0.2 dB low. The ratio of measured-to-calculated transmission loss therefore should be decreased by 0.8 dB. The specific attenuation is slightly higher at 7.74 GHz and using a ratio of 1.2 of the total zenith attenuation from a point on the surface for 7.74 GHz relative to the total attenuation at 4.5 GHz (surface curve on Fig. 1, Ref. 6) a correction of 1.0 dB is required for the X-band data (including the correction for the L-band radar data). Rain will also cause attenuation along the path. Noting that in the summer the radar data typically displayed rain cells less than 5 km across in the region of high Z_e value (45 to 55 dBZ), the rain attenuation is less than 0.4 dB at C-band (see Ref. 12 for relationship between Z and specific attenuation) and may be neglected. At X-band, the same cell (50 dBZ, 5 km across) would cause 3.3 dB additional attenuation along the path.

A corrected table of comparisons was generated using the Doppler spread and gaseous absorption correction values to correct the comparison data and is presented in Table VI. Attenuation due to rain was not considered in making the corrections. Table VI provides the best estimated comparison values within the assumptions of single scattering theory, Rayleigh scatter

TABLE VI
CORRECTED HISTOGRAM COMPARISONS RATIO OF MEASURED-TO-CALCULATED
TRANSMISSION LOSS

Description	Compare	Mode (dB)	Median (dB)	Mean* (dB)	RMS (dB)	No. of Samples
C-band Rain – Summer 1970 within clear lines-of-sight and –10 dB directivity	6-sec avg.	+2	+2	+1.2 ± 0.4	3.7	661
C-band Rain – Summer 1970 within clear lines-of-sight	6-sec avg.	+2	0	–0.1 ± 0.4	4.7	1206
C-band Rain – Summer 1970 all data above 0.7° Avon horizon angle	6-sec avg.	+2	0	+0.8 ± 0.4	6.3	2388
X-band Rain – Summer 1968 within clear lines-of-sight and –10 dB directivity	6-sec avg.	–2	–2	–1.6 ± 0.5	3.2	450
X-band Rain – Summer 1968 within clear lines-of-sight	6-sec avg.	–2	–2	–1.0 ± 0.5	4.0	539
X-band Rain – Summer 1968 all data above 0.7° Avon horizon angle	6-sec avg.	–2	0	+2.3 ± 0.7	8.5	1529
C-band Turbulence, Fall 1970	6-sec avg.	–1	–1	–0.8 ± 1.2	5.0	164
C-band Snow, Fall 1970	scan	+2	+2	+2.1 ± 0.7	1.4	38

* Range of possible values is $\pm 3\sigma$.

for spheres, and no hydrometeor attenuation as used in interference computations for the CCIR. The mean logarithm of the ratio of measured-to-computed transmission loss values presented in Table VI is within the 2.7-dB maximum ratio estimation uncertainty (3σ) quoted in Table IV for the 1970 measurements and the 3.7-dB uncertainty for the 1968 measurements. Within the measurement and computation accuracy of the Avon-to-Westford experiment, the computational model predicted the measured transmission loss values.

B. Discussion of Results, Hydrometeor Scatter

The hydrometeor and cloud particle computational model was based upon the assumption that the scattering particles were spherical. The analysis of hydrometeor scattering given in Section 2.1.3 of Ref. 5 discussed corrections to the model both for spherical particles larger than about $1/10$ wavelength (Mie Scattering) and for spheroidal particles in the Rayleigh Scattering limit. For backscattering, the ratio of the Mie theory (exact) and the Rayleigh theory (approximate) estimate of scattering from an ensemble of water spheres has a value of -0.1 dB at L-band (1.3 GHz, the radar frequency), -0.6 dB at C-band (4.5 GHz, the frequency used for bi-static scatter during 1970), and $+1.3$ dB at X-band (7.74 GHz, the frequency used for bistatic scatter during 1968) for the Laws and Parsons¹³ drop size distribution and a 152 mm/hr rain rate ($Z = 57$ dBZ). For lower rain rates the differences between Mie and Rayleigh theory are smaller (see Table VII). The corrections to Rayleigh theory required to adequately describe backscattering from water spheres at high Z values are within a half dB of the residual difference listed in the Table. The Z_e values for the rain cells used in the comparison analysis ranged from $20 \leq Z_e \leq 55$ and, at 27 dBZ, the ratio of Mie to Rayleigh Z_e values is -0.2 dB at C-band and -0.3 dB at X-band indicating that this explanation for the residual differences is only partially correct. The ratio of (mZ_e) to (mZ) for Mie scattering is scattering angle dependent. For C-band, the scattering angle dependence is small causing less than ± 0.8 dB difference over the range of scattering angles used for a Z value of 46 dBZ (see Fig. 12, Ref. 5). For X-band, the difference between the Mie and Rayleigh theory prediction for scattering from water spheres is

TABLE VII
CORRECTIONS TO Z VALUES FOR BACKSCATTER FOR THE EXACT
(Mie) SOLUTION FOR SCATTERING FROM SPHERES

Rate (mm/hr)	Z (dBZ)	$\frac{Z_e}{Z}$ at 1.30 GHz (dB)	$\frac{Z_e}{Z}$ at 4.52 GHz (dB)	$\frac{Z_e}{Z}$ at 7.75 GHz (dB)
0.25	17.4	0.0	-0.1	-0.2
1.27	27.5	0.0	-0.2	-0.3
2.5	31.9	0.0	-0.2	-0.2
12.7	41.6	0.0	-0.4	+0.2
25	45.9	-0.1	-0.5	+0.5
51	50.1	-0.1	-0.6	+0.8
102	54.2	-0.1	-0.6	+1.1
152	56.7	-0.1	-0.6	+1.3

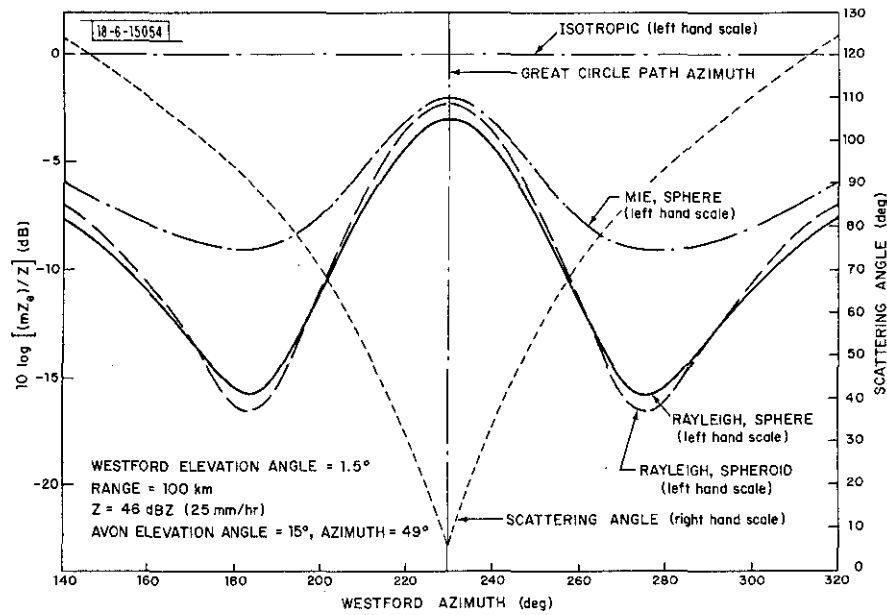


Fig. 28. $(mZ_e)/Z$ for Rayleigh and Mie scattering theories for water spheres and Rayleigh scattering theory for water spheroids, horizontal-to-circular polarization, Avon-to-Westford scatter path.

TABLE VIII CORRECTIONS TO Z VALUES FOR BACKSCATTER FROM VERTICALLY ORIENTED OBLATE SPHEROIDS				
Rate (mm/hr)	Z (dBZ)	$\frac{Z_{eRL}}{Z}$ at 1.295 GHz* (dB)	$\frac{Z_{VV}}{Z}$ at 4.515 GHz (dB)	$\frac{Z_{HL}}{Z}$ at 7.74 GHz (dB)
0.25	17.4	-0.06	-0.27	+0.14
1.27	27.5	-0.12	-0.55	+0.31
2.5	31.9	-0.14	-0.71	+0.41
12.7	41.6	-0.18	-1.07	+0.64
25	45.9	-0.20	-1.27	+0.78
51	50.1	-0.21	-1.44	+0.89
102	54.2	-0.22	-1.62	+1.01
152	56.7	-0.22	-1.72	+1.07

* R, L, V, H represent right-hand circular, left-hand circular, vertical, and horizontal polarization, respectively, with the first letter for the transmitted polarization and second for received.

more pronounced. For the polarizations and range of pointing angles used, the difference may be as large as 6 dB as shown in Fig. 28 for Westford azimuth angles between 260° and 280°.

Observations of scattering from hydrometeors below the melting layer with multiple polarization radars have indicated that rain particles are not water spheres but behave as oblate spheroids with a vertical symmetry axis.^{14,15} An analysis of scattering from vertically oriented spheroids in the Rayleigh limit using the Laws and Parsons drop mass relationships and the shape distribution proposed by Pruppacher and Pitter¹⁶ was given in Section 2.1.3 of Ref. 5. Using a similar analysis, for backscatter at the measurement frequencies, the corrections listed in Table VIII are obtained. These corrections if applied to the transmission loss values would also reduce the differences between the observed and calculated values for the summer rain showers. The corrections for bistatic scattering for X-band and the range of scattering angles used in the Avon-to-Westford experiment are shown in Fig. 28 for a rain rate of 25 mm/hr (46 dBZ) and a Westford elevation angle of 1.5°. The results are within 1 dB of the values listed for Rayleigh scattering from a sphere. At C-band, the correction for scattering from vertically oriented spheroids at a 25 mm/hr rain rate is within 0.3 dB of the value for backscatter listed in Table VIII ($\varphi = 180^\circ$) for the range of scattering angles displayed in Fig. 28.

The computations of possible differences from the simple Rayleigh scattering from spheres model are not useful for a further refining of the computations of transmission loss because no information about the hydrometeor state is available. These computations show that the possible corrections are small at C-band and would tend to improve the comparison both at C- and at X-band.

The measurements of scattering from snow and cirrostratus clouds made during the fall of 1970 do not agree with the calculations as well as the summer hydrometeor scatter data. The cirrus cloud transmission loss measurements were 5 to 6 dB higher (lower received signal) than the computations predicted (7 to 8 dB before correction). The snow scattering measurements were 2 dB higher than the computations predicted. Although the difference between the calculation and measurements for snow are smaller than the possible error in estimating the difference (ratio), the differences for cirrostratus clouds were larger. The data indicate that the simple Rayleigh approximation for spheres, while useful for snow, does not hold as well for scattering from the ice particles within a cirrus cloud. Scattering from cirrostratus clouds is quite weak and of little consequence in interference estimation problems.

Two forms of hydrometeor scatter that may both be of importance as a cause of interference and show departure from the simple Rayleigh sphere scatter model used above are melting snow and hail. Hail was not observed during any of the measurement periods. Melting snow (bright band) was observed on the radar during the fall measurement period but the melting layer was not high enough to be observed bistatically with clear lines-of-sight and no melting layer data were obtained. Melting layers were also observed in dissipating rain cells during the summer months. The number of observations was small and any departure from the assumed model for calculation would cause an increase in the observed rms value for the ratios of measured-to-calculated transmission loss.

C. Discussion of Results, Turbulent Scatter

Useful data for comparison were only obtained during the fall of 1970. Comparisons were made for single scans for the summer data and presented as a part of the preliminary data analysis (see Refs. 3 and 4). The preliminary analysis showed apparent agreement within the system

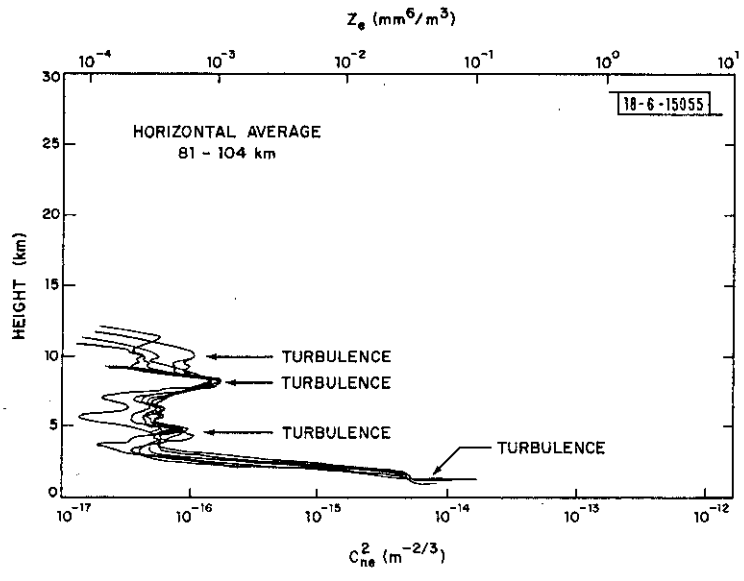


Fig. 29. C_{ne}^2 profile, Millstone Hill radar, 229.0-229.5° azimuth, 1507-1534 GMT, 28 October 1970.

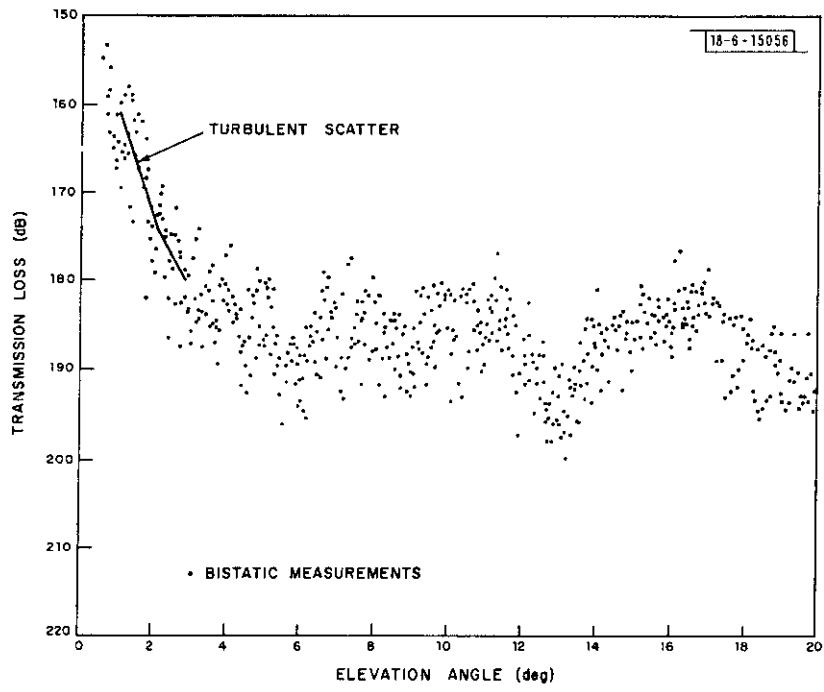


Fig. 30. Calculated and measured transmission loss, Avon-to-Westford scatter path, 229.0-229.5° azimuth (Westford), 1510-1514 and 1527-1534 GMT, 28 October 1970; Avon: 3° elevation, 49° azimuth, 4-foot antenna, vertical polarization.

measurement errors but insufficient data were obtained to prepare a comparison histogram. The data from 2 November 1970 showed agreement between the bistatically measured transmission loss and the predictions based upon the theory of turbulent scatter for refractive index fluctuations in the inertial subrange (see Ref. 2). The corrected mean ratio of measured-to-calculated transmission loss was -0.8 ± 1.2 dB which is well within the system measurement error of 2.7 dB.

The data used for the comparison histogram (Fig. 18) were for turbulent layers that coexisted with low level stratus clouds. These layers were among the strongest detected during the measurement period ($C_{ne}^2 \sim 6 \times 10^{-14} \text{ m}^{-2/3}$). On clear days the layer strengths especially at several km above the surface were much weaker as shown in Fig. 29. Figure 30 gives the simultaneous C-band bistatic measurements. The data have a similar variation in transmission loss with elevation angle as the 2 November 1970 data with the exception of approximately a 15 dB lower scattered signal at a Westford elevation angle of $1-1.75^\circ$ and 20 dB lower signal (higher transmission loss) at an elevation angle of 2.5° .

Turbulent scatter was detected in the direction of the great circle path on each measurement day. The scattered signal could be separated from the stronger great circle path signal at low elevation angle for elevation or azimuth angles within 3° of the angle of arrival of the stronger signal (also due to turbulent scatter). At larger elevation or azimuth offset angles, sidelobe coupling always occurred. The scattering from turbulence observed during the measurement periods always had the scattering angle and Doppler shift characteristics attributable to refractive index fluctuations in the inertial subrange. The shape of the spectrum could depart slightly from the $-11/3$ slope characteristic of the 3-dimensional power spectral density in the inertial subrange region of wavenumber space for the refractive index fluctuations [the slope determines the wavelength and scattering angle dependence of Eq. (12)] and not be detected by this experiment. Other observers have noted both turbulent scatter as described above (volume filled turbulence) and a quasi-specular form of (turbulent) scatter from very thin layers or "feuillets."^{17,18} This latter form of turbulent scatter was not observed in this experiment.

On several of the days, strong ducted (anomalous propagation) returns were observed on the L-band radar at ranges comparable to the surface distance between Avon and Westford and from the azimuth of the great circle path. During these conditions, no enhancement in the turbulent scattered signals was detected. The natural terrain shielding at Avon apparently reduced coupling into the duct sufficiently to cause signals propagated via that mode to not be detectable in comparison with the turbulent scatter signal.

VI. CONCLUSIONS

Observations were made of coupling between two stations located on the surface of the earth caused by rain scatter and turbulent scatter. Simultaneous radar observations were made in the scattering volumes and used together with the bistatic radar equation and simplified approximate descriptions of the scattering process to calculate the coupling (transmission loss) between the two stations. For scattering by rain, snow, or refractive index fluctuations (turbulence), the simplified models predicted the measured values within the measurement accuracies of both the monostatic and bistatic radars. The computational procedures used by the CCIR (Ref. 1) therefore are adequate for the hydrometeor types observed. The C- and X-band measurements for rain produced nearly identical results indicating that for the prediction of interference due to rain, the effects of attenuation do not have to be considered for frequencies less than or equal to 7.74 GHz.

ACKNOWLEDGMENT

The author wishes to acknowledge the help and support of the staff of the Millstone Hill radar site and the staff of the Westford Communications site. Messrs. B. E. Nichols and H. H. Hoover of the latter site contributed much to the program. The effort of Mrs. Louise M. Balboni, who was responsible for the data processing programs, is also gratefully acknowledged.

The Westford and Millstone Hill facilities are supported by the Department of the Air Force under Contract F19628-73-C-0002.

REFERENCES

1. CCIR Report 339-1 (Rev. 72), "Influence of Scattering from Precipitation on the Siting of Earth and Terrestrial Stations," and Report AC/5, "Simplified Propagation Model for the Determination of Coordination Distance in the Frequency Range 1-40 GHz," Conclusions of the Interim Meeting of Study Group 5, Propagation in Non-Ionized Media (International Telecommunications Union, Geneva, 1972).
2. V. I. Tatarski, Wave Propagation in a Turbulent Medium (McGraw-Hill, New York, 1961).
3. R. K. Crane, "A Comparison Between Monostatic and Bistatic Scattering from Rain and Thin Turbulent Layers," Technical Note 1970-29, Lincoln Laboratory, M.I.T. (6 October 1970), DDC AD-N71-12395.
4. R. K. Crane, "Description of the Avon-to-Westford Experiment," Technical Report 483, Lincoln Laboratory, M.I.T. (29 April 1971).
5. R. K. Crane, "Virginia Precipitation Scatter Experiment - Data Analysis," GSFC Doc. X-750-73-55, NASA, Goddard Space Flight Center (November 1972).
6. R. K. Crane, "Propagation Phenomena Affecting Satellite Communication Systems Operating in the Centimeter and Millimeter Wavelength Bands," Proc. IEEE 59, 173-188 (1971).
7. H. Goldstein, Classical Mechanics, Sec. 4-4 (Addison-Wesley, Mass., 1959).
8. D. Atlas, "Advances in Radar Meteorology," Sec. 3.5.5 Advances in Geophysics, Vol. 10, ed. by H. E. Landsberg and J. Van Miegham (Academic Press, New York, 1964).
9. R. K. Crane, "Measurement of Clear Air Turbulence in the Lower Stratosphere Using the Millstone Hill L-Band Radar," Preprints, 14th Weather Radar Conference, pp. 101-106, Amer. Meteorol. Soc., Boston, Mass., November 1970.
10. A. S. Dennis, "The Scattering of SHF Radio Waves by Hail and Wet Snow," Final Report NASA Contract NASr-49(02), Stanford Research Institute, Menlo Park, Calif., June 1964.
11. J. S. Marshall, and W. Hirschfeld, "Interpretation of the Fluctuating Echo from Randomly Distributed Scatterers, Part I," Can. J. Phys. 31, 962 (1953).
12. R. K. Crane, "Microwave Scattering Parameters for New England Rain," Technical Report 426, Lincoln Laboratory, M.I.T. (3 October 1966), DDC AD-647798.
13. J. O. Laws and D. A. Parsons, "The Relationship of Raindrop-Size to Intensity," Am. Geophys. Unions Trans. 24, 452-460 (1943).
14. G. C. McCormick and A. Hendy, "Results of Precipitation Backscatter Measurements at 1.8 cm with a Polarization Diversity Radar," Preprints 15th Weather Radar Conference, pp. 35-38, Amer. Meteorol. Soc., Boston, Mass., October 1972.
15. G. C. McCormick and A. Hendy, "The Study of Precipitation Backscatter at 1.8 cm with a Polarization Diversity Radar," Preprints 14th Weather Radar Conference, Amer. Meteorol. Soc., Boston, Mass., November 1970.
16. H. R. Pruppacher and R. L. Pitter, "A Semi-Empirical Determination of the Shape of Cloud and Rain Drops," J. of Atmospheric Sci. 28, 86-94 (1971).
17. F. DeCastel, Tropospheric Radiowave Propagation Beyond the Horizon (Pergamon Press, New York, 1966).
18. W. P. Birkemeier, A. B. Fontaine, I. H. Gerks, and R. D. Pittle, "Troposcatter Signal Characteristics Simulated by Random Layered Scatterer Arrays," Radio Sci. 4, 1225-1223 (1969).